antipyretic effects. Rat and mouse P450s primarily metabolize ketoprofen to hydroxyketoprofen.[6,7] In humans, ketoprofen is primarily metabolized by UDP-glucuronosyltransferase (UGT) and is converted to ketoprofen glucuronides.[8] Recently, it was demonstrated that when chimeric mice were administered ketoprofen, glucuronide conjugates were detected in their sera and bile. However, these conjugates are minor products; ketoprofen was primarily hydrolyzed in mice, and the main metabolites were hydrolyzed ketoprofen and glucuronide-conjugated ketoprofen.[7]

The metabolism of chemical entities has been examined using animals in the laboratory, but this approach fails to address differences in drug metabolism that exist between animal species. Because of the species differences in metabolic abilities, fresh h-hepatocytes are a better model for predicting the metabolism of drugs in the human body. For technical reasons, preparing fresh h-hepatocytes ahead of time and performing reproducible studies using the same donor are not possible. Thus, cryopreserved h-hepatocytes have been used, but they are compromised on thawing, resulting in decline and alteration of their normal function. Additionally, h-hepatocytes exhibit large individual differences in P450 activities. The differences might be due to real individual differences and/or the cryopreserving and thawing conditions.

We hypothesized that these practical problems in using h-hepatocytes for in vitro drug testing could be addressed if h-hepatocytes isolated from chimeric mouse livers exhibited human-type drug metabolism capacities in vitro. In the present study, we first determined the yield, viability, and purity of isolated h-hepatocytes from chimeric mice (chimeric hepatocytes). We compared the P450 activities of fresh and cryopreserved chimeric hepatocytes and assessed glucuronide activities toward ketoprofen using fresh and cryopreserved chimeric hepatocytes and cryopreserved donor hepatocytes.

We demonstrate that the chimeric mouse liver is a useful tool that can supply fresh hepatocytes retaining high P450 and UGT activities and allowing reproducible assays using hepatocytes derived from the same donor.

Materials and Methods

Materials: Phenacetin, tolbutamide, *S*-mephenytoin, dextromethorphan, chlorzoxazone, testosterone, ketoprofen, and Krebs-Henseleit buffer (KHB) were purchased from Sigma-Aldrich (St. Louis, MO). Coumarin and midazolam were obtained from Wako Pure Chemical Industries (Osaka, Japan). All other chemicals and solvents were of the highest or analytical grade commercially available.

Generation of mice with humanized livers: The present study was approved by the ethics committee of PhoenixBio Co., Ltd. and the Hiroshima Prefectural Institute of Industrial Science and Technology Ethics Board.

Cryopreserved h-hepatocytes from three donors (4YF, a 4-year-old Caucasian girl; 6YF, a 6-year-old African-American girl; and 2YM, a 2-year-old Caucasian boy) were purchased from BD Biosciences (San Jose, CA). Three (donor 4YF), 17 (donor 6YF), and 4 (donor 2YM) chimeric mice with humanized livers, generated by a method described previously, were used.[1] The concentration of human albumin (hAlb) in the blood of the chimeric mice and the replacement index (RI, the rate of hepatocyte replacement from mouse to human) were well correlated.[1] In the current study, we used 11–15-week-old male and female chimeric mice with approximately 11–14 mg/mL hAlb in mouse blood (RI > 70%); uPA/SCID mice were used as controls.

Isolation of hepatocytes from chimeric mouse liver, SCID mouse liver, and human liver tissue: Hepatocytes were isolated from the 4YF-, 6YF-, and 2YM-chimeric mice using a two-step collagenase perfusion method. The liver was perfused at 38 °C for 10 min at 1.5 mL/min with Ca^{2+}-free and Mg^{2+}-free Hanks' balanced salt solution (CMF-HBSS) containing 200 mg/mL ethylene glycol tetraacetic acid (EGTA), 1 mg/mL glucose, 10 mM *N*-2-hydroxyethylpiperazine-*N*′-2-ethanesulfonic acid (HEPES), and 10 μg/mL gentamicin. The perfusion solution was then changed to CMF-HBSS containing 0.05% collagenase (Wako Pure Chemical Industries), 0.6 mg/mL $CaCl_2$, 10 mM HEPES, and 10 μg/mL gentamicin, and perfusion was continued for 17–23 min at 1.5 mL/min. The liver was dissected and transferred to a dish; liver cells were gently disaggregated in the dish with CMF-HBSS containing 10% bovine Alb, 10 mM HEPES, and 10 μg/mL gentamicin. The disaggregated cells were centrifuged three times (50 × *g*, 2 min). The pellet was suspended in medium consisting of Dulbecco's modified Eagle's medium (DMEM), 10% fetal bovine serum (FBS), 20 mM HEPES, 44 mM $NaHCO_3$, and antibiotics (100 IU/mL penicillin G and 100 μg/mL streptomycin). Cell number and viability were assessed using the trypan blue exclusion test.

Normal liver tissues were obtained from the resected liver of nine patients (51-, 53-, and 64-year-old men and a 68-year-old woman for plating efficiency; 54-, 57-, and 75-year-old men for P450 activity; and 55- and 69-year-old women for screening of monoclonal antibodies) after receiving consent prior to surgery, in accordance with the 1975 Declaration of Helsinki. Hepatocytes were isolated via two-step collagenase perfusion and low-speed centrifugation.[1] Aliquots of freshly isolated hepatocytes from four individuals, used for determining plating efficiency, were suspended at $1–2 \times 10^7$ cells/mL/vial in cryopreservation solution (Cellbanker; Juji Field, Inc., Tokyo, Japan), cryopreserved using a program freezer (Kryo-10 Series III; Planer Products Ltd., Sunbury-on-

Thames, Middlesex, UK), and kept in liquid nitrogen. To measure the plating efficiency of the hepatocytes, 4YF-chimeric hepatocytes and hepatocytes from human livers were inoculated onto 13.5-mm Celldesks (Sumitomo Bakelite, Tokyo, Japan) in 24-well plates (BD Biosciences) for 24 h, followed by fixation with ethanol and staining with hematoxylin and eosin. Adhered hepatocytes were counted under the microscope and plating efficiency was calculated by dividing number of adhered cells by the cell number inoculated in a well.

Hepatocytes were isolated from three male uPA (wt/wt)/SCID mice by collagenase perfusion methods.[9] They were used for *in vitro* glucuronidation activity studies.

Purification of h-hepatocytes from total hepatocytes of the chimeric mouse livers: A Fischer 344 rat was immunized intraperitoneally three times (once a week) with 10^7 mouse hepatocytes (m-hepatocytes) of SCID mice as an antigen, and injected with a booster of 2.5×10^7 m-hepatocytes at 3 weeks after the last immunization. Hybridomas were obtained by conventional methods and screened on immunohistochemical sections using m- and h- (from a 55-year-old woman) liver tissues. Frozen h- and m- liver sections were incubated with hybridoma supernatants and fluorescein-labeled anti-rat IgG antibodies (Alexa Fluor 594; Molecular Probes, Eugene, OR). Supernatants from 10 hybridoma clones were reacted with the plasma membrane of m-hepatocytes, but not with h-hepatocytes on the sections. The reactivity of each of the supernatants to the cell surface was determined with a fluorescence-activated cell sorter (FACS) as follows. Isolated m- and h- (69-year-old woman) hepatocytes were incubated with the supernatants and fluorescein isothiocyanate (FITC)-conjugated second antibodies (Alexa Fluor 488; Molecular Probes) and analyzed with a FACS Vantage SE (BD Biosciences) using a 100-μm nozzle. Fluorescence excited at 488 nm was measured through a 530-nm filter (FL1) with 4-decade logarithmic amplification. A hybridoma clone was selected as the clone that produced antibodies reactive to the cell surface of m-hepatocytes, but not h-hepatocytes. The antibody was purified from the culture medium of the hybridoma cells by protein G affinity column or ion exchange chromatography; the antibody was named 66Z.

Isolated h-hepatocytes from chimeric mice were contaminated with m-hepatocytes. To remove the m-hepatocytes, 6YF-hepatocytes isolated from the chimeric mice were incubated with the 66Z antibody, washed with DMEM containing 10% FBS, and incubated with Dynabeads M450-conjugated sheep anti-rat IgG (Dynal Biotech, Milwaukee, WI) in a tube for 30 min on ice. The tube was placed in Dynal MPC-1 (Dynal Biotech) for 1–2 min to remove 66Z-positive ($66Z^+$) m-hepatocytes. Enriched h-hepatocytes were collected as 66Z-negative ($66Z^-$) cells. Aliquots of chimeric hepatocytes from before and after enrichment were incubated with FITC-conjugated 66Z antibodies, and the proportion of $66Z^+$-cells in the h-hepatocytes was determined by FACS.

***In vitro* metabolic study using hepatocytes and microsomes:** For the measurement of the P450 activities of four fresh and five cryopreserved 6YF-chimeric mice, cryopreserved donor cells (6YF), and fresh h-hepatocytes from three individuals, suspended hepatocytes (6×10^4 cells) were incubated in KHB with each of eight substrates specific for seven P450 subtypes (phenacetin for CYP1A2, coumarin for CYP2A6, tolbutamide for CYP2C9, *S*-mephenytoin for CYP2C19, dextromethorphan for CYP2D6, chlorzoxazone for CYP2E1, and midazolam and testosterone for CYP3A) in 96-well plates (BD Biosciences) for 1 or 2 h (**Table 1**). The incubated solution was collected and an equivalent volume of methanol containing 1 μM niflumic acid (internal standard) was added. After centrifugation (10,000 rpm), the supernatant was subjected to liquid chromatography-tandem mass spectrometry (LC-MS/MS) (MDS SCIEX; Applied Biosystems, Foster City, CA). The LC system consisted of an HP 1100 system including a binary pump, an automatic sampler, and a column oven (Agilent Technologies, Waldbronn, Germany), equipped with a Symmetry Shield C18 column (Waters, Tokyo, Japan). The column temperature was 35°C. The mobile phase was 40% acetonitrile/0.1% formic acid (v/v). The flow rate was 0.3 mL/min. The LC was connected to a PE Sciex API2000 tandem mass spectrometer (Applied Biosystems), operated in positive electrospray ionization mode. The turbo gas was maintained at 550°C. Nitrogen was used as the nebulizing gas, turbo gas, and curtain gas at 65, 85, and 30 psi, respectively. Parent and/or fragment ions were filtered in the first quadrupole and dissociated in the collision cell using nitrogen as the collision gas. The analytical conditions for each substrate are shown in **Table 2**. The experiments were performed in triplicate per mouse, and the results are expressed as the average value of three mice or humans.

To assess changes in the P450 activities of fresh and cryopreserved 2YM-chimeric hepatocytes during storage at 4°C for 3 and 6 h, fresh and cryopreserved chimeric hepatocytes were prepared from two 2YM chimeric mice. The isolated hepatocytes from the chimeric mice were purified by isodensity centrifugation (27% Percoll, 7 min, 4°C) to remove dead hepatocytes. Cells (4×10^5 cells) were incubated in KHB with four different substrates specific for four P450s (phenacetin for CYP1A2, diclofenac for CYP2C9, *S*-mephenytoin for CYP2C19, and midazolam for CYP3A) in 24-well plates (BD Biosciences) for 2 h (**Table 1**). The incubated solution was collected and the concentration of the metabolites was measured by high-performance liquid chromatography (HPLC; Lachome Elite; Hitachi High-Technology Co., Tokyo, Japan). HPLC was performed at

Table 1. Reaction conditions for determination of CYP activities using cells and microsomes for LC-MS/MS and HPLC analysis

Enzymes measured	Enzyme activity	Substrate (concentration, mM)	Metabolite	Cells (LC-MS/MS)	Cells (HPLC)	Microsomes (LC-MS/MS)	
				Incubation time (h)	Incubation time (h)	Buffer*	Incubation time (min)
CYP1A2	Phenacetin *O*-deethylase	Phenacetin (15)	Acetaminophen	2	2	PB	20
CYP2A6	Coumarin 7-hydroxylase	Coumarin (8)	7-Hydroxycoumarin	2	–	TB	20
CYP2C9	Tolbutamide 4-hydroxylase	Tolbutamide (150)	Hydroxytolbutamide	2	–	TB	10
	Diclofenac 4′-hydroxylase	Diclofenac (100)	4-Hydroxydiclofenac	–	2	–	–
CYP2C19	*S*-Mephenytoin 4′-hydroxylase	*S*-Mephenytoin (20)	(±)-4′-Hydroxymephenytoin	2	2	PB	20
CYP2D6	Dextromethorphan *O*-demethylase	Dextromethorphan (8)	Dextrorphan	2	–	PB	20
CYP2E1	Chlorzoxazone 6-hydroxylase	Chlorzoxazone (100)	6-Hydroxychlorzoxazone	2	–	PB	20
CYP3A	Midazolam 1′-hydroxylase	Midazolam (10)	1′-Hydroxymidazolam	1	2	PB	10
	Testosterone 6β-hydroxylase	Testosterone (50)	6β-Hydroxytestosterone	2	–	PB	10

*TB, Tris-HCl buffer (pH 7.5); PB, potassium phosphate buffer (pH 7.4).

Table 2. Analytical parameters of LC-MS/MS for CYP1A2, 2A6, 2C9, 2C19, 2D6, 2E1, and 3A assays

Enzymes measured	Analyte	Mass spectrometer conditions						
		Mode	Declustering potential (eV)	Collision energy (eV)	Entrance potential (eV)	Collision cell exit potential (eV)	Ionspray voltage (V)	Analyte *m/z* transition
CYP1A2	Acetaminophen	Positive	40	25	7	10	5000	152.2→110.3
CYP2A6	7-Hydroxycoumarin	Positive	80	30	7	10	4200	162.8→107.2
CYP2C9	Hydroxytolbutamide	Positive	40	25	7	10	5000	286.9→171.3
CYP2C19	(±)-4′-Hydroxymephenytoin	Positive	80	25	7	10	4200	234.9→150.1
CYP2D6	Dextrorphan	Positive	120	40	7	10	4200	259.0→200.2
CYP2E1	6-Hydroxychlorzoxazone	Negative	−80	−25	−7	−10	−4200	184.1→120.0
CYP3A	6β-Hydroxytestosterone	Positive	60	25	7	10	4200	305.9→270.3
	1′-Hydroxymidazolam	Positive	100	40	7	10	5000	341.6→203.3
Ketoprofen	Ketoprofen	Positive	80	35	7	10	5000	255.5→104.9

a flow rate of 1.0 mL/min using the CAPCELL PAK C18, UG120 (4.6×250 mm, 5 μm; Shiseido, Tokyo, Japan) for CYP1A2 and CYP2C19, Inertsil ODS-3 (4.6×250 mm, 5 μm; GL Sciences Inc., Tokyo, Japan) for CYP2C9, and Xterra RP18 (4.6×150 mm, 5 μm; Waters) for CYP3A. Other analytical conditions are shown in **Table 3**. The measurements were performed in duplicate.

Liver microsomes were prepared from a 6YF-chimeric mouse and control uPA/SCID mice as described previously.[10] They were stored at −80°C until analysis. The protein concentration was determined using a Bradford protein assay kit (Bio-Rad, Hercules, CA), using bovine serum albumin as the standard. Microsomes from a chimeric mouse liver, pooled microsomes of six uPA/SCID mice, and pooled microsomes of 20 human livers (BD Gentest; BD Biosciences) were incubated with the substrates at 37°C for 5 min following incubation with the reduced form of nicotinamide adenine dinucleotide phosphate (NADPH) cofactor solution (3.8 mM β-$NADP^+$, 9.7 mM glucose-6-phosphate, 9.7 mM $MgCl_2$, 1.2 U/mL glucose-6-phosphate dehydrogenase) at 37°C for 10 or 20 min (**Table 1**). The incubated solution was collected and the concentration of the metabolites was measured by LC-MS/MS. The experiments were performed in triplicate per microsome preparation, and the results are expressed as the average value.

Detection of CYP2A6 gene mutations by the Invader assay: CYP2A6 polymorphism was determined by BML, Inc. (Tokyo, Japan). Genomic DNA was isolated from thawed human hepatocytes and the DNA was used

Table 3. Analytical conditions of HPLC for CYP1A2, 2C9, 2C19, and 3A assays

Enzymes measured	Analyte	Internal standard	Injection volume (μL)	Mobile phase				
				Solvent A*	Solvent B	Gradient program, %B (min)	Column temperature (°C)	UV detection (nm)
CYP1A2	Acetaminophen	0.1 μg Caffeine monohydrate	95	50 mM PB (pH 4.0)	Acetonitrile	Isocratic mode (A/B = 91/9)	35	245
CYP2C9	4′-Hydroxydiclofenac	0.4 μg Phenacetin	50	0.5% (v/v) AAAS	Methanol containing 0.5% (v/v) acetic acid	40 (0)→90 (30) →90 (35)→40 (36)	50	280
CYP2C19	(±)-4′-Hydroxymephenytoin	0.1 μg Phenobarbital sodium	95	50 mM PB	Acetonitrile	Isocratic mode (A/B = 80/20)	35	240
CYP3A	1′-Hydroxymidazolam	0.01 μg Phenacetin	50	10 mM PB (pH 7.4)	Acetonitrile/methanol mixture (7/5, v/v)	30 (0)→30 (5)→60 (17) →60 (25)→30 (26)	40	263

*PB, potassium phosphate buffer; AAAS, acetic acid aqueous solution.

for determining CYP2A6 polymorphism by the Invader assay.[11]

***In vitro* glucuronidation activity study using hepatocytes:** Ketoprofen metabolism was examined using three types of hepatocytes: fresh and cryopreserved 6YF-chimeric hepatocytes, cryopreserved donor cells (6YF), and fresh uPA(wt/wt)/SCID mouse hepatocytes. Hepatocytes (4×10^5 cells) suspended in KHB were plated in 24-well, non-treated plates (BD Biosciences) and incubated at 37 °C for 15 min. The cells were treated with 1 μM ketoprofen at 37 °C for 3 h. The medium was harvested and aliquots of the medium were incubated at 37 °C for 4 h with 0.25 M acetic acid buffer as a solvent control (A) and with 2500 units/mL β-glucuronidase (B). Equivalent 1 N KOH was added into (B) and incubated at 80 °C for 3 h (C). After incubation, an equivalent of methanol containing 1 μM niflumic acid (as an internal standard) was added. After centrifugation (10,000 rpm), the supernatant was subjected to LC-MS/MS.

The relevant concentrations can then be obtained:

[Concentration of ketoprofen in (B)] − [Concentration of ketoprofen in (A)] gives [Concentration of ketoprofen-glucuronide].

[Concentration of ketoprofen in (C)] − [Concentration of ketoprofen in (B)] gives [Concentration of transferred ketoprofen-glucuronide].

The transferred ketoprofen is the acyl glucuronide positional isomer, formed by acyl migration, which may be the glucuronide form transferred from ketoprofen-glucuronide during incubation. The experiments were performed in triplicate for a given mouse, and the results are expressed as the average value of three chimeric mice for fresh chimeric hepatocytes, the average of five chimeric mice for cryopreserved hepatocytes, and the average of three uPA(wt/wt)/SCID mice for fresh control mouse hepatocytes.

Statistics: The data were analyzed using Statcel2 (OMS Publishing Inc., Tokorozawa, Japan). Results are expressed as the mean ± SD, and the significance of the difference between two groups was analyzed by Student's *t*-test when data were normally distributed, and by Welch's *t*-test otherwise. $P < 0.05$ was deemed to indicate statistical significance.

Results

Yield, viability, and plating efficiency of isolated h-hepatocytes: Hepatocytes from the 4YF-, 6YF-, and 2YM-donors were transplanted into uPA/SCID mice, and chimeric mice were obtained bearing the respective donor hepatocytes (**Table 4**). The chimeric mice (4YF, 3 mice; 6YF, 17 mice; 2YM, 4 mice) were sacrificed at 54–83 days post-transplantation (**Table 4**). On the day they were sacrificed, blood was collected for the determination of hAlb concentrations (**Table 4**). Hepatocytes were then isolated by the collagenase perfusion method. Numbers (yield) of isolated viable hepatocytes were approximately $2–3 \times 10^7$ cells/mouse (**Table 4**). The viabilities were approximately 60–70% and 50–60% for fresh and cryopreserved chimeric hepatocytes, respectively, without Percoll purification.

The plating efficiency of hepatocytes from the chimeric mice was about 66.6 ± 3.4% (mean ± SD), while those of fresh hepatocytes and cryopreserved hepatocytes from human livers were 34.0 ± 19.3% and 9.3 ± 8.3%, respectively.

Purification of h-hepatocytes isolated from chimeric mice: Chimeric hepatocyte preparations consisted of h- and m-hepatocytes. It was found that 17.3 ± 6.7% of the fresh hepatocytes from 6YF-chimeric mice were $66Z^+$ ($n = 4$; **Table 4**) by FACS analysis. The enriched chimeric hepatocytes were found to be 3.3 ± 1.0% $66Z^+$ (m-hepatocytes; $n = 4$; **Table 4**).

P450 activities of hepatocytes from the chimeric mice: The P450 activities of hepatocytes from 6YF-chi-

Table 4. Hepatocytes used for the experiments

Purpose	Origin	Fresh or cryopreserved	n (sex of host animals or patients)	hAl in mouse blood (mg/mL)	Yield of hepatocytes ($\times 10^7$ cells)	Viability (%)	Ratio of mouse hepatocytes (%)	
							Before purification	After purification
Plating efficiency	Chimeric mouse (4YF)	Fresh	3 (M: 1, F: 2)	11.5±3.6	2.90±2.7/mouse	63.9±6.5	N.D.[*4]	N.D.
	Human liver (51–68-year-old)	Fresh	4 (M: 3, F: 1)	–	0.98±0.4/g liver	87.9±8.2	–	–
		Cryopreserved	4 (M: 3, F: 1)	–	–	56.2±7.5[*5]	–	–
CYP activities	Chimeric mouse (6YF)	Fresh	4[*1] (F)	11.8±0.6	1.78±0.9/mouse	61.8±6.9	17.3±6.7	3.3±1.0
		Cryopreserved	5[*2] (M: 2, F: 3)	12.6±2.1	–	60.5±10.6[*5]	5.8±4.7[*5]	2.1±1.0[*5]
	Human liver (54–75-year-old)	Fresh	3 (M: 3)	–	0.43±0.4/g liver	96.1±2.4	–	–
	Donor cell (6YF)	Cryopreserved	1 (F)	–	–	71.1	–	–
CYP activities at different time points after perfusion or thawing	Chimeric mouse (2YM)	Fresh	2[*3] (F)	11.8	3.05[*5),6]/mouse	84.8[*5),6]	N.D.	N.D.
		Cryopreserved	2[*3] (F)	11.8	–	86.4[*5),6]	N.D.	N.D.
Glucuronide activities	Chimeric mouse (6YF)	Fresh	3 (F)	13.5±2.9	3.24±1.0/mouse	69.8±11.2	9.8±2.0	–
		Cryopreserved	5 (M: 3, F: 2)	13.4±2.4	–	50.7±5.1[*5]	12.5±7.2	–
	Donor cell (6YF)	Cryopreserved	1 (F)	–	–	86.7	–	–
	uPA (wt/wt)/SCID mouse	Fresh	3	–	1.51±0.3/mouse	73.2±4.7	–	–

[*1] Hepatocytes from one of four mice were used for CYP1A2, 2C9, and 3A (testosterone), and those from another were used for CYP2A6, 2C19, 2D6, 2E1, and 3A (midazolam). Hepatocytes from two mice were used for all tested P450s.
[*2] Hepatocytes from one of five mice were used for CYP1A2, 2C9, and 3A (testosterone); those from a second mouse were used for CYP2A6, 2C19, and 2E1; those from a third mouse were used for CYP2C19, 2D6, 3A (midazolam); and those from a fourth mouse were used for tested P450s except for CYP2C19. Those from a fifth mouse were used for all tested P450s.
[*3] Hepatocytes from one of two mice were used for CYP1A2 and 3A, and those from the second mouse were used for CYP2C9 and 2C19.
[*4] Not determined.
[*5] Data after thaw.
[*6] Data after purification with Percoll.

meric mice were determined using eight substrates (**Table 1**). The reactions of P450 activities with all substrates shown in **Table 1** were linear with incubation time. The activities of fresh chimeric hepatocytes were compared with cryopreserved chimeric hepatocytes and cryopreserved donor cells. Three experiments were performed and the means±SD are given in **Figure 1**. CYP1A2, 2C19, and 2D6 activities in fresh chimeric hepatocytes were approximately twice those in cryopreserved cells (**Fig. 1**). CYP2A6, 2C9, 2E1, and 3A activities in fresh chimeric hepatocytes were similar to those of cryopreserved hepatocytes (**Fig. 1**). The activities of cryopreserved donor cells (6YF) were lower than those of cryopreserved 6YF-chimeric hepatocytes in CYP1A2, 2C19, and 3A (midazolam); higher in CYP2A6 and 2E1; and similar in CYP2C9, 2D6, 3A (testosterone; **Fig. 1**). Compared with CYP2A6 activities of two of the three fresh hepatocytes, CYP2A6 activity was extremely low in the chimeric hepatocytes (**Fig. 1**). Interestingly, the Invader assay revealed that donor 6YF had the *1/*4 CYP2A6 polymorphism; livers with the *1/*4 polymorphism in CYP2A6 are known to show low CYP2A6 activity.[12] We concluded that the low CYP2A6 activity was due to the *1/*4 polymorphism of donor 6YF. Three kinds of fresh h-hepatocytes were also examined for P450 activity. One of the three samples did not show CYP1A2 or 2C19 activity. Large individual differences were observed among the three in CYP2A6, 2C9, and 2E1 activities. The activities of CYP1A2, 2C19, 2D6, and 3A in fresh h-hepatocytes were lower than those in fresh chimeric hepatocytes.

We determined changes in the P450 activities of fresh and cryopreserved 2YM-chimeric hepatocytes after Percoll purification during storage at 4°C after isolation and thawing, respectively. CYP1A2, 2C9, 2C19, and 3A activities did not change for up to 6 h after isolation or thawing (**Fig. 2**). CYP1A2, 2C19, and 3A activities were lower in cryopreserved chimeric hepatocytes, and CYP2C9 activity was similar compared to fresh chimeric hepatocytes at 0 h after isolation or thawing (**Fig. 2**). The results were reproducible and are similar to those in **Figure 1**.

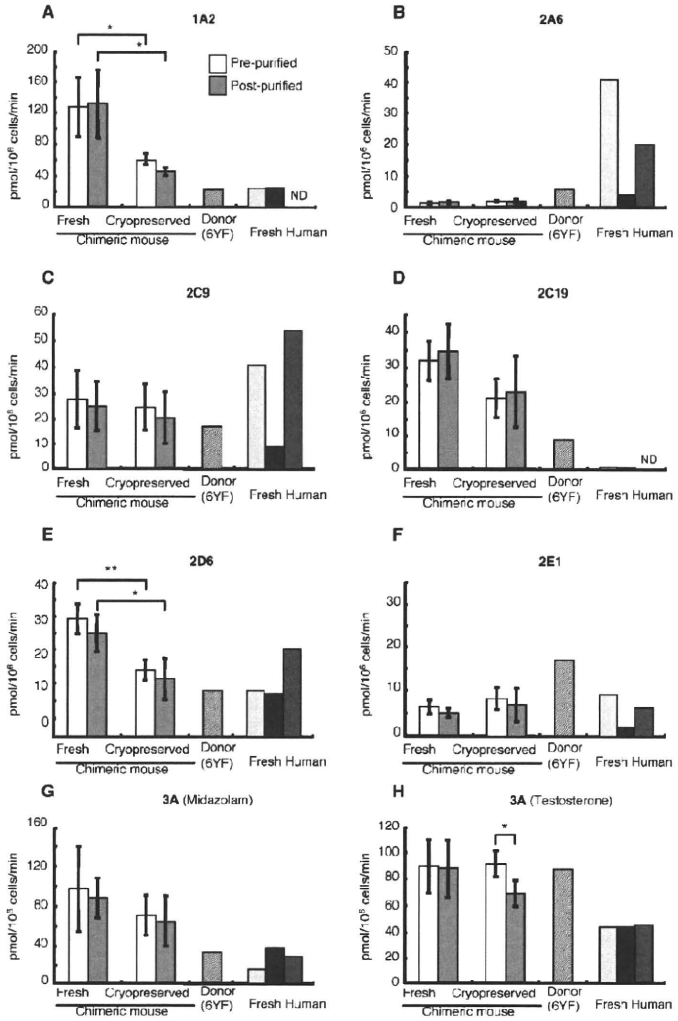

Fig. 1. P450 activities of fresh and cryopreserved chimeric hepatocytes, cryopreserved donor hepatocytes, and fresh h-hepatocytes, determined by LC-MS/MS

Hepatocytes were isolated from 6YF-chimeric mice. Aliquots of the isolated hepatocytes were frozen with a programmed freezer. Aliquots of fresh and thawed cryopreserved chimeric hepatocytes were purified with 66Z antibodies by magnetic sorting. Cryopreserved donor hepatocytes (6YF) for the chimeric mice were thawed. Fresh h-hepatocytes were isolated from resected livers after surgery from three patients. Eight kinds of suspended hepatocytes were incubated with eight substrates specific for seven P450s (Table 1): (A) 1A2, (B) 2A6, (C) 2C9, (D) 2C19, (E) 2D6, (F) 2E1, (G) 3A, midazolam, and (H) 3A, testosterone. The incubated medium was analyzed for each metabolite by LC-MS/MS (Table 2) and the metabolic activity of each P450 is shown as pmol/10^6 cells/min. Data in fresh and cryopreserved chimeric hepatocytes are shown as means ± SD of metabolite concentrations of three different chimeric mice. $^*p < 0.05$, $^{**}p < 0.01$. ND, not detected.

Contribution of m-hepatocyte contamination in chimeric hepatocytes to P450 activity: The proportions of m-hepatocytes in the fresh chimeric hepatocytes were approximately 17% and 3% before and after purification with 66Z antibodies, respectively, as described above. To determine how the contaminating m-hepatocytes affected P450 activities, we measured P450 activities using liver microsomes from a 6YF-chimeric mouse, pooled host uPA/SCID mice, and pooled human liver microsomes. Except for CYP2D6 and 2E1, P450 activities were similar or lower in uPA/SCID mouse liver microsomes than in human pooled microsomes (**Fig. 3**). Because the activities of CYP2D6 and 2E1 in uPA/SCID mouse liver microsomes were 50–100% higher than in pooled human microsomes (**Fig. 3**), we considered that m-hepatocytes contaminating the chimeric hepatocytes at around 17% might not significantly affect the activities of chimeric hepatocytes. We measured the P450 activity of pre- and post-purified chimeric hepatocytes (6YF) using 66Z antibodies. The purified hepato-

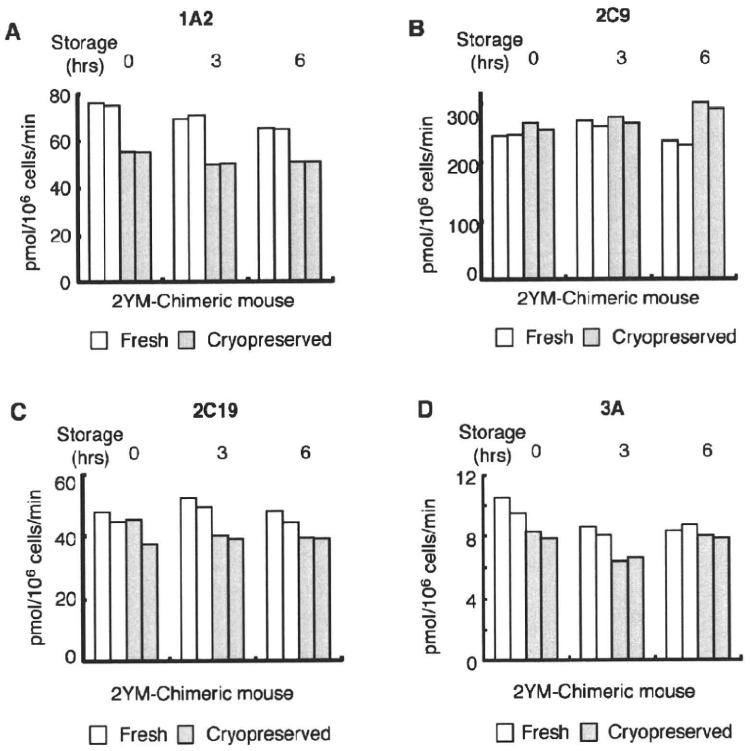

Fig. 2. Time course of P450 activities in fresh and cryopreserved chimeric hepatocytes after isolation or thawing, respectively, as assessed by HPLC

Fresh and cryopreserved 2YM-chimeric hepatocytes were stored after isolation and thawing, respectively, at 4°C for 3 and 6 h. The fresh and cryopreserved chimeric hepatocytes were purified by Percoll isodensity centrifugation after isolation or thawing. Fresh and cryopreserved chimeric hepatocytes, just after purification (0 h) and after storage for 3 h and 6 h, were treated with four substrates specific for four P450s (Table 1): (A) 1A2, (B) 2C9, (C) 2C19, and (D) 3A. The incubated medium was used to analyze each metabolite by HPLC; the metabolic activity of each P450 is shown as pmol/10^6 cells/min (Table 3).

cytes from the chimeric mice showed similar P450 activities to unpurified ones, supporting this suggestion (**Fig. 1**).

Glucuronide conjugation of ketoprofen in chimeric m-hepatocytes: Glucuronide conjugates were detected by *in vitro* metabolic assay for ketoprofen using fresh and cryopreserved hepatocytes from the 6YF-chimeric mouse and cryopreserved donor cells (6YF); however, uPA(wt/wt)/SCID mouse hepatocytes did not show products of UGT activity. The proportion of non-metabolized ketoprofen in fresh chimeric hepatocytes was similar to that in donor cells and lower than that in cryopreserved chimeric hepatocytes (**Fig. 4**). The proportion of ketoprofen-glucuronide in fresh chimeric hepatocytes was significantly higher than that of both cryopreserved chimeric hepatocytes ($P<0.05$). The transferred ketoprofen-glucuronide levels in fresh chimeric hepatocytes were also higher than those of both cells, but not significantly so (**Fig. 4**). From these results, we suggest that the freeze-thaw procedure decreased cellular glucuronide conjugation activities on drugs such as ketoprofen.

Discussion

Recent studies have revealed that chimeric mice may be a useful model for the examination of drug absorption, distribution, metabolism, and excretion (ADME) and drug interactions via enzyme induction and inhibition *in vivo*.[1,3,4,7,12-14] S-Warfarin has been shown to be metabolized to S-7-hydroxywarfarin, catalyzed by CYP2C9, and is primarily recovered in urine in humans.[15] The mass balance and metabolic disposition of S-warfarin in chimeric mice were found to be similar to reported human data.[14,16] In humans, ketoprofen is primarily metabolized by UGT and converted to ketoprofen glucuronides.[8] When chimeric mice were administered ketoprofen, glucuronide conjugates were detected in their sera and bile.[7] By treatment with typical inducers of P450 (3-methylcholanthrene and rifampicin), human CYP1A and CYP3A4, respectively, were induced in the chimeric mouse liver.[1,3] After treatment with quinidine, a specific inhibitor of human CYP2D6, the area under the curve (AUC) of CYP2D6 metabolites was significantly decreased in the chimeric mice, but not in

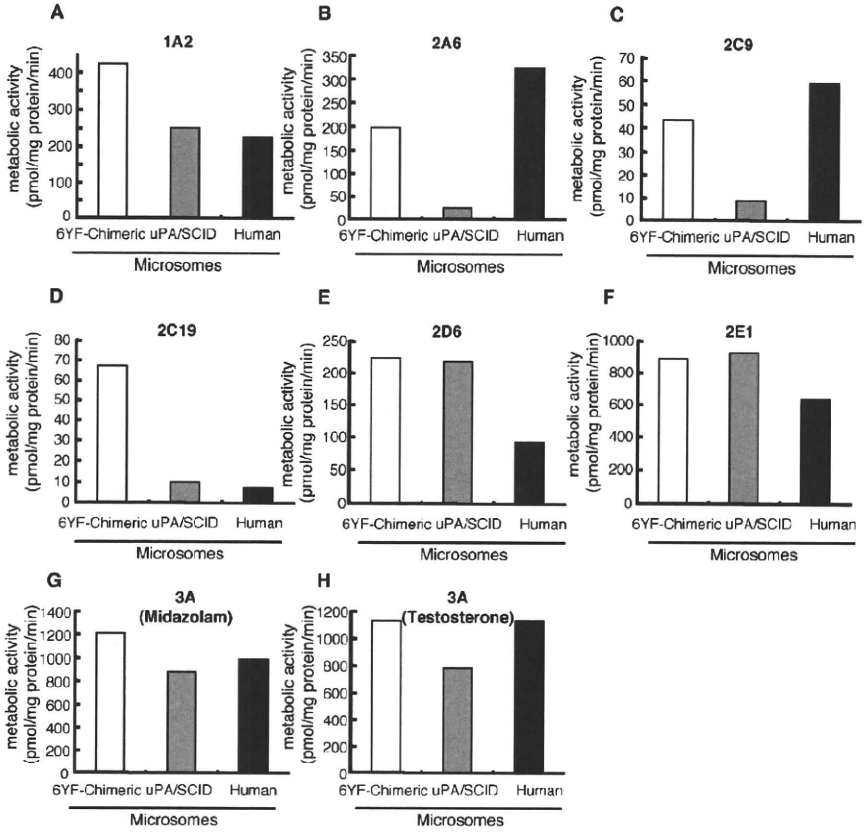

Fig. 3. P450 activities of liver microsomes from chimeric mice, uPA/SCID mice, and human livers as determined by LC-MS/MS
Microsomes from a 6YF-chimeric mouse and pooled microsomes of uPA/SCID mice and human livers were treated with eight substrates specific for seven P450s (Table 1), and the metabolite concentrations were measured by LC-MS/MS; the metabolic activity of each P450 is shown as pmol/mg protein/min (Table 2): (A) 1A2, (B) 2A6, (C) 2C9, (D) 2C19, (E) 2D6, (F) 2E1, (G) 3A, midazolam, and (H) 3A, testosterone.

control mice.[13] These findings demonstrate that h-hepatocytes in the chimeric mouse liver had normal human phase I and II enzyme activity, and that the chimeric mice may have advantages in studies of ADME and drug interactions. However, no study had examined the metabolic activity of fresh h-hepatocytes isolated from chimeric mice. In the present study, we determined whether the chimeric mouse could be a useful source of fresh h-hepatocytes for *in vitro* metabolic studies.

The metabolic capacities of fresh and corresponding cryopreserved hepatocytes from several donors have been compared by testosterone hydroxylation, 7-ethoxyresorufin-*O*-deethylase (EROD), and 7-ethoxycoumarin-*O*-deethylase (ECOD). These activities were found to be lower in cryopreserved hepatocytes than in fresh ones.[17,18] Phase II enzyme activities, GST, UGT toward 4-methylumbelliferone (MUF), and sulfotransferase (SULT) were also significantly reduced after cryopreservation of h-hepatocytes, whereas the activity of UGT toward 4-hydroxybiphenyl (HOBI) and that of SULT were similar to those measured in fresh h-hepatocytes.[17] Despite the observed reductions of these enzyme activities, cryopreserved h-hepatocytes are regarded as the best *in vitro* model for use in predicting human intrinsic clearance of xenobiotics.[19] This is because ahead-of-time experimental planning using fresh h-hepatocytes and attaining reproducible studies using the same donor of fresh h-hepatocytes is not feasible. Additionally, because large individual variations are known to exist among h-hepatocytes, pooled hepatocytes derived from several donors could help eliminate such individual variation, but such pooling of fresh h-hepatocytes is not possible. Here, we compared the P450 activities of fresh and cryopreserved chimeric hepatocytes originating from the same donor, and fresh h-hepatocytes from human livers. Results indicated that CYP1A2, 2C19, and 2D6 activities declined, while CYP2A6, 2C9, 2E1, and 3A activities were not affected by the freeze-thaw procedure. Fresh and cryopreserved chimeric h-hepatocytes were used for the determination of ketoprofen glucuronidation. Concentrations of ketoprofen-glucuronide and transferred ketoprofen-glucuronide were higher in fresh chimeric hepatocytes than in their cryopreserved counterparts. Chimeric hepatocytes from the same donor showed

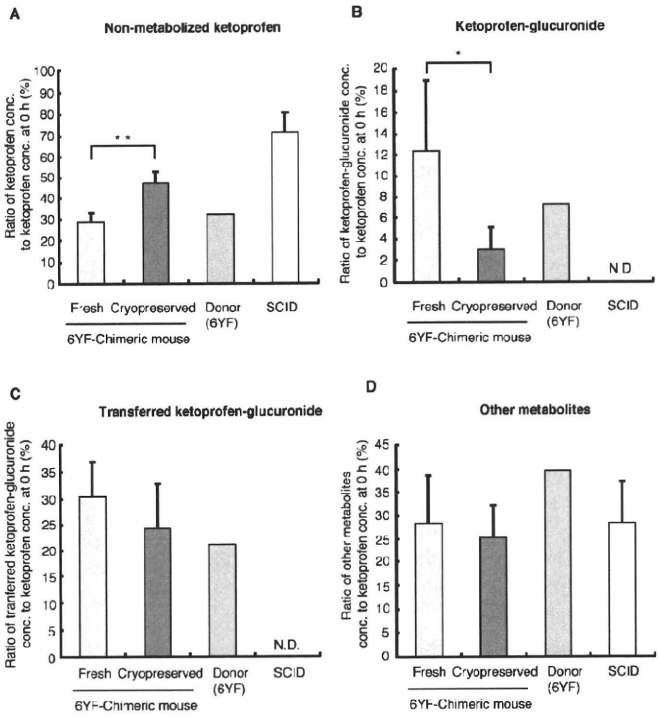

Fig. 4. Glucuronidation of ketoprofen in fresh and cryopreserved chimeric hepatocytes, uPA(wt/wt)/SCID mouse hepatocytes, and cryopreserved donor hepatocytes, as determined by LC-MS/MS

Fresh and cryopreserved chimeric hepatocytes, uPA(wt/wt)/SCID mouse hepatocytes, and cryopreserved donor hepatocytes (6YF) were incubated with ketoprofen for 3 h. The conditioned medium was treated with β-glucuronidase and 1 N KOH, and the concentration of ketoprofen was measured by LC-MS/MS (Table 2): (A) Non-metabolized ketoprofen, (B) Ketoprofen-glucuronide, (C) Transferred ketoprofen-glucuronide, and (D) other metabolites. The concentrations of ketoprofen-glucuronide and transferred ketoprofen-glucuronide were calculated by the formulas indicated in Materials and Methods, and the activities were expressed as the ratio of the concentration of ketoprofen or its glucuronide conjugate to the ketoprofen concentration at 0 h. The values shown are the means ± SD of three or five different chimeric mice. $^{*}p<0.05$, $^{**}p<0.01$. ND, not detected.

smaller variations in P450 activities than fresh h-hepatocytes from different individuals (**Fig. 1**). These results indicated that fresh chimeric hepatocytes may address the problem of individual differences in fresh h-hepatocytes. Additionally, the fresh and cryopreserved chimeric hepatocytes tested retained P450 (CYP1A2, 2C9, 2C19, and 3A) activities for at least 6 h. These studies demonstrated that chimeric mice can provide fresh h-hepatocytes ahead of time, making reproducible studies using the same donor possible.

The decreased metabolism in cryopreserved hepatocytes could be attributable to two mechanisms: inactivation of P450 enzymes and loss of the cofactor NADPH due to cell membrane damage.[20] The addition of a NADPH-generating system to the incubation mixture has been shown to increase benzo[a]pyrene metabolite formation by cryopreserved rat hepatocytes to approximately the level of freshly isolated rat hepatocytes.[21] When cryopreserved rat hepatocytes were purified by Percoll centrifugation after thawing, to remove dead and membrane-damaged cells, benzo[a]pyrene metabolism recovered to equal that of fresh rat hepatocytes.[21] The decline in phase II enzyme activities has also been shown to be overcome by Percoll centrifugation, but not completely to the level of freshly isolated cells.[21] Addition of endogenous cofactors uridine 5′-diphosphoglucuronic acid (UDPGA) and adenosine 3′-phosphate 5′-phosphosulfate (PAPS) to cryopreserved rat hepatocytes improved 7-hydroxycoumarin-glucuronide and 7-hydroxycoumarin-sulfate formation to levels observed in fresh hepatocytes.[22] The UDPGA and PAPS synthesis machineries may be damaged during freezing and thawing. Fresh or cryopreserved chimeric hepatocytes would be useful in clarifying the mechanisms underlying the decline in metabolic activities after freezing and thawing. The results of this study also suggest that fresh chimeric hepatocytes are useful for testing phase I and II reactions, including glucuronidation, without the need for Percoll purification or the addition of cofactors.

Chimeric hepatocytes contain about 17% of m-hepatocytes, and 66Z antibodies react specifically with m-hepatocytes. We purified h-hepatocytes from the chimer-

ic hepatocytes by 66Z rat IgG and magnetic bead-conjugated anti-rat IgG antibodies. After the magnetic removal of m-hepatocytes, the proportion of m-hepatocytes decreased to approximately 3%. We measured the P450 activities of microsomes isolated from the chimeric mouse and pooled microsomes from uPA/SCID mice and human livers using the same substrates as those used in the cell suspension study. Because we were not able to obtain microsomes from the donor of the chimeric mice (6YF), pooled human microsomes were used for this study. Except for CYP2D6 and 2E1, the activities of uPA/SCID mouse liver microsomes were similar to, or lower than, those of pooled human liver microsomes. The activities of CYP2D6 and 2E1 in uPA/SCID mouse liver microsomes were 50–100% higher than those of pooled human liver microsomes, respectively. We also found that P450 activities were similar between pre- and post-purified chimeric hepatocytes. From these results, we deduced that m-hepatocytes contaminating the chimeric hepatocytes might not significantly affect the activities of chimeric hepatocytes.

Gender differences in CYP3A4 activities have been reported when using cryopreserved human hepatocytes.[23] We assumed that P450 activities were independent of the gender in recipient uPA/SCID mice, because we recently showed that there was no significant difference in P450 activity (CYP1A2, 2C9. 2C19, 2D6, and 3A) between microsomes from male and female chimeric mice.[24] In the present study, hepatocytes isolated from both male and female chimeric mice were used, and there was no difference in P450 or UGT activity between them (data not shown); however, the number of animals was limited.

Non-platable 4YF- and 6YF-donor cells were engrafted and grown in the uPA/SCID mice and hepatocytes were isolated from the livers using the collagenase perfusion method. Fresh chimeric hepatocytes adhered well onto the culture dishes, compared with fresh and cryopreserved h-hepatocytes. This suggests that fresh chimeric hepatocytes would be suitable for P450 induction and toxicity studies that are usually performed with plated cells.

Cryopreserved h-hepatocytes isolated from the chimeric mice were demonstrated to be useful for evaluating the induction of CYP1A2 and 3A4;[25] in addition, CYP1A2 and 3A4 mRNA induction and expression from three different donor hepatocytes were reproduced in cryopreserved chimeric hepatocytes.[26] Due to the higher plating efficiency of fresh hepatocytes compared to cryopreserved cells, fresh chimeric hepatocytes would be useful for evaluating the human P450 induction abilities of xenobiotics.

We conclude that fresh and reproducible h-hepatocytes isolated from chimeric mice could be a useful tool in predicting the pharmacokinetics of chemical entities in addition to *in vivo* chimeric mouse studies. Comparative *in vitro* and *in vivo* studies using chimeric mice with the same donor could generate abundant data for resolving poorly understood phenomena and mechanisms.

Acknowledgments: We thank Mss. Y. Yoshizane, S. Nagai, and H. Kohno for providing excellent technical assistance.

References

1) Tateno, C., Yoshizane, Y., Saito, N., Kataoka, M., Utoh, R., Yamasaki, C., Tachibana, A., Soeno, Y., Asahina, K., Hino, H., Asahara, T., Yokoi, T., Furukawa, T. and Yoshizato, K.: Near completely humanized liver in mice shows human-type metabolic responses to drugs. *Am. J. Pathol.*, **165**: 901–912 (2004).
2) Katoh, M., Matsui, T., Nakajima, M., Tateno, C., Kataoka, M., Soeno, Y., Horie, T., Iwasaki, K., Yoshizato, K. and Yokoi, T.: Expression of human cytochrome P450 in chimeric mice with humanized liver. *Drug Metab. Dispos.*, **32**: 1402–1410 (2004).
3) Katoh, M., Matsui, T., Nakajima, M., Tateno, C., Soeno, Y., Horie, T., Iwasaki, K., Yoshizato, K. and Yokoi, T.: In vivo induction of human cytochrome P450 enzymes expressed in chimeric mice with humanized liver. *Drug Metab. Dispos.*, **33**: 754–763 (2005).
4) Katoh, M., Matsui, T., Okumura, H., Nakajima, M., Nishimura, M., Naito, S., Tateno, C., Yoshizato, K. and Yokoi, T.: Expression of human phase II enzymes in chimeric mice with humanized liver. *Drug Metab. Dispos.*, **33**: 1333–1340 (2005).
5) Wilkinson, G. R.: Drug metabolism and variability among patients in drug response. *N. Engl. J. Med.*, **352**: 2211–2221 (2005).
6) Populaire, P., Terlain, B., Pascal, S., Decouvelaere, B., Renard, A. and Thomas, J. P.: Biological behavior: serum levels, excretion and biotransformation of (3-benzoylphenyl)-2-propionic acid, or ketoprofen, in animals and men. *Ann. Pharm. Fr.*, **12**: 735–749 (1973).
7) Hashizume, K., Ohzone, Y., Adachi, Y., Ninomiya, A., Inoue, T. and Horie, T.: Characterization of chimeric mouse on in vivo metabolism of ketoprofen. *The Cell*, **40**: 26–29 (2008) in Japanese.
8) Ishizaki, T., Sasaki, T., Suganuma, T., Horai, Y., Chiba, K., Watanabe, M., Asuke, W. and Hoshi, H.: Pharmacokinetics of ketoprofen following single oral, intramuscular and rectal doses and after repeated oral administration. *Eur. J. Clin. Pharmacol.*, **18**: 407–414 (1980).
9) Ohashi, K., Tatsumi, K., Utoh, R., Takagi, S., Shima, M. and Okano, T.: Engineering liver tissues under the kidney capsule site provides therapeutic effects to hemophilia B mice. *Cell Transplant.*, in press
10) Sugihara, K., Kitamura, S., Yamada, T., Ohta, S., Yamashita, K., Yasuda, M. and Fujii-Kuriyama, Y.: Aryl hydrocarbon receptor (Ah)-mediated induction of xanthine oxidase/xanthine dehydrogenase activity by 2,3,7,8-tetrachlorodibenzo-p-dioxin. *Biochem. Biophys. Res. Commun.*, **281**: 1093–1099 (2001).
11) Nagano, M., Yamashita, S., Hirano, K., Ito, M., Maruyama, T., Ishihara, M., Sagehashi, Y., Oka, T., Kujiraoka, T., Hattori, H., Nakajima, N., Egashira, T., Kondo, M., Sakai, N. and Matsuzawa, Y.: Two novel missense mutations in the CETP gene in Japanese hyperalphalipoproteinemic subjects: high-throughput

assay by Invader assay. *J. Lipid Res.*, **43**: 1011–1018 (2002).
12) Kiyotani, K., Yamazaki, H., Fujieda, M., Iwano, S., Matsumura, K., Satarug, S., Ujjin, P., Shimada, T., Guengerich, F. P., Parkinson, A., Honda, G. Nakagawa, K., Ishizaki, T. and Kamataki, T.: Decreased coumarin 7-hydroxylase activities and CYP2A6 expression levels in humans caused by genetic polymorphism in CYP2A6 promoter region (CYP2A6*9). *Pharmacogenetics*, **13**: 689–695 (2003).
13) Katoh, M., Sawada, T., Soeno, Y., Nakajima, M., Tateno, C., Yoshizato, K. and Yokoi, T.: *In vivo* drug metabolism model for human cytochrome P450 enzyme using chimeric mice with humanized liver. *J. Pharm. Sci.*, **96**: 428–437 (2007).
14) Inoue, T., Nitta, K., Sugihara, K., Horie, T., Kitamura, S. and Ohta, S.: CYP2C9-catalyzed metabolism of S-warfarin to 7-hydroxywarfarin *in vivo* and *in vitro* in chimeric mice with humanized liver. *Drug Metab. Dispos.*, **36**: 2429–2433 (2008).
15) Rettie, A. E., Korzekwa, K. R., Kunze, K. L., Lawrence, R. F., Eddy, A. C., Aoyama, T., Gelboin, H. V., Gonzalez, F. J. and Trager, W. F.: Hydroxylation of warfarin by human cDNA-expressed cytochrome P-450: a role for P-4502C9 in the etiology of (S)-warfarin-drug interactions. *Chem. Res. Toxicol.*, **5**: 54–59 (1992).
16) Inoue, T., Sugihara, K., Ohshita, H., Horie, T., Kitamura, S. and Ohta, S.: Prediction of human disposition toward S-3H-warfarin using chimeric mice with humanized liver. *Drug Metab. Pharmacokinet.*, **24**: 153–160 (2009).
17) Steinberg, P., Fischer, T., Kiulies, S., Biefang, K., Platt, K. L., Oesch, F., Bottger, T., Bulitta, C., Kempf, P. and Hengstler, J.: Drug metabolizing capacity of cryopreserved human, rat, and mouse liver parenchymal cells in suspension. *Drug Metab. Dispos.*, **27**: 1415–1422 (1999).
18) Gebhardt, R., Hengstler, J. G., Muller, D., Glöckner, R., Buenning, P., Laube, B., Schmelzer, E., Ullrich, M., Utesch, D., Hewitt, N., Ringel, M., Hilz, B. R., Bader, A., Langsch, A., Koose, T., Burger, H. J., Maas, J. and Oesch, F.: New hepatocyte in vitro systems for drug metabolism: metabolic capacity and recommendations for application in basic research and drug development, standard operation procedures. *Drug Metab. Rev.*, **35**: 145–213 (2003).
19) Lau, Y. Y., Sapidou, E., Cui, X., White, R. E. and Cheng, K. C.: Development of a novel in vitro model to predict hepatic clearance using fresh, cryopreserved, and sandwich-cultured hepatocytes. *Drug Metab. Dispos.*, **30**: 1446–1454 (2002).
20) Hengstler, J. G., Utesch, D., Steinberg, P., Platt, K. L., Diener, B., Ringel, M., Swales, N., Fischer, T., Biefang, K., Gerl, M., Böttger, T. and Oesch, F.: Cryopreserved primary hepatocytes as a constantly available in vitro model for the evaluation of human and animal drug metabolism and enzyme induction. *Drug Metab. Rev.*, **32**: 81–118 (2000).
21) Diener, B., Utesch, D., Beer, N., Dürk, H. and Oesch, F.: A method for the cryopreservation of liver parenchymal cells for studies of xenobiotics. *Cryobiology*, **30**: 116–127 (1993).
22) Wang, Q., Jia, R., Ye, C., Garcia, M., Li, J. and Hidalgo, I. J.: Glucuronidation and sulfation of 7-hydroxycoumarin in liver matrices from human, dog, monkey, rat, and mouse. *In Vitro Cell Dev. Biol. Anim.*, **41**: 97–103 (2005).
23) Parkinson, A., Mudra, D. R., Johnson, C., Dwyer, A. and Carroll, K. M.: The effects of gender, age, ethnicity, and liver cirrhosis on cytochrome p450 enzyme activity in human liver microsomes and inducibility in cultured human hepatocytes. *Toxicol. Appl. Pharmacol.*, **199**: 193–209 (2004).
24) Kikuchi, R., McCown, M., Olson, P., Tateno, C., Morikawa, Y., Katoh, Y., Bourdet, D. L., Monshouwer, M. and Fretland, A. J.: Effect of hepatitis C virus infection on the mRNA expression of drug transporters and cytochrome p450 enzymes in chimeric mice with humanized liver. *Drug Metab. Dispos.*, **38**: 1954–1961 (2010).
25) Nishimura, M., Yokoi, T., Tateno, C., Kataoka, M., Takahashi, E., Horie, T., Yoshizato, K. and Naito, S.: Induction of human CYP1A2 and CYP3A4 in primary culture of hepatocytes from chimeric mice with humanized liver. *Drug Metab. Pharmacokinet.*, **20**: 121–126 (2005).
26) Yoshitsugu, H., Nishimura, M., Tateno, C., Kataoka, M., Takahashi, E., Soeno, Y., Yoshizato, K., Yokoi, T. and Naito, S.: Evaluation of human CYP1A2 and CYP3A4 mRNA expression in hepatocytes from chimeric mice with humanized liver. *Drug Metab. Pharmacokinet.*, **21**: 465–474 (2006).

Molecular Cell
Article

Methionine Adenosyltransferase II Serves as a Transcriptional Corepressor of Maf Oncoprotein

Yasutake Katoh,[1,2] Tsuyoshi Ikura,[1,6] Yutaka Hoshikawa,[3] Satoshi Tashiro,[4] Takashi Ito,[5] Mineto Ohta,[1] Yohei Kera,[1] Tetsuo Noda,[3] and Kazuhiko Igarashi[1,2,*]
[1]Department of Biochemistry
[2]Center for Regulatory Epigenome and Diseases
Tohoku University Graduate School of Medicine, Sendai, Miyagi 980-8575, Japan
[3]Genome Center, Japanese Foundation for Cancer Research, Kotoku, Tokyo 135-8550, Japan
[4]Department of Cellular Biology, RIRBM, Hiroshima University, Hiroshima 734-8553, Japan
[5]Department of Biochemistry, Nagasaki University School of Medicine, Nagasaki 852-8523, Japan
[6]Present address: Department of Mutagenesis, Radiation Biology Center, Kyoto University, Kyoto 606-8501, Japan
*Correspondence: igarashi@med.tohoku.ac.jp
DOI 10.1016/j.molcel.2011.02.018

SUMMARY

Protein methylation pathways comprise methionine adenosyltransferase (MAT), which produces *S*-adenosylmethionine (SAM) and SAM-dependent substrate-specific methyltransferases. However, the function of MAT in the nucleus is largely unknown. MafK represses or activates expression of heme oxygenase-1 (HO-1) gene, depending on its heterodimer partners. Proteomics analysis of MafK revealed its interaction with MATIIα, a MAT isozyme. MATIIα was localized in nuclei and found to form a dense network with chromatin-related proteins including Swi/Snf and NuRD complexes. MATIIα was recruited to Maf recognition element (MARE) at HO-1 gene. When MATIIα was knocked down in murine hepatoma cell line, expression of HO-1 was derepressed at both basal and induced levels. The catalytic activity of MATIIα, as well as its interacting factors such as MATIIβ, BAF53a, CHD4, and PARP1, was required for HO-1 repression. MATII serves as a transcriptional corepressor of MafK by interacting with chromatin regulators and supplying SAM for methyltransferases.

INTRODUCTION

Metabolic flux regulation by compartmentalization of enzymes and substrate channeling is a common theme in many enzymatic pathways. It is becoming clear that some metabolic enzymes related to gene regulation are compartmentalized in nuclei (Hall et al., 2004; Takahashi et al., 2006; Wellen et al., 2009). For example, yeast acetyl-CoA synthetase-2 (ACS2), which catalyzes the synthesis of metabolic intermediate acetyl-CoA, is present in nuclei to provide acetyl-CoA for histone acetylation (Takahashi et al., 2006). Another metabolic intermediate important for gene regulation is obviously *S*-adenosylmethionine (SAM) as a methylation donor (Lu and Mato, 2008). Methylation at cytosine of DNA and at arginine and lysine residues of various proteins including histones are catalyzed by specific methyltransferases using SAM as a methyl donor (Dillon et al., 2005; Goll and Bestor, 2005; Shi, 2007). In contrast to the case of nuclear protein acetylation, how SAM is provided to nuclear methyltransferases is not clear.

Methionine adenosyltransferase (MAT) is a cellular enzyme that catalyzes the formation of SAM from methionine and ATP. Three distinct forms of MAT (MATI, MATII, and MATIII), encoded by two distinct genes (*MAT1A* and *MAT2A*), have been identified in mammals (Sakata et al., 1993, 2005). MATI and MATIII are a tetramer and a dimer, respectively, of α_1 catalytic subunit, which is encoded by *MAT1A*. MATIIα, the catalytic subunit of MATII, is encoded by *MAT2A* and forms a dimer, and its activity is inhibited by MATIIβ regulatory subunit encoded by *MAT2B*. While MATI/III is expressed at high levels in adult liver, MATIIα is widely expressed (Kotb et al., 1997; Halim et al., 2001; LeGros et al., 2001). While MATI/III have been reported to be present in nuclei (Reytor et al., 2009), function of MATI/III or MATII in terms of gene regulation is not yet clear.

The small Maf oncoproteins, MafG, MafK, and MafF, possess a basic region-leucine zipper (bZip) domain for dimer formation and DNA binding (Fujiwara et al., 1993; Kataoka et al., 1995; Igarashi et al., 1995). They repress or activate transcription depending on the dimeric partner. For example, MafK-Bach1 heterodimer and MafK-p45 heterodimer (i.e., NF-E2) serve as a repressor and an activator of globin genes, respectively, during erythroid differentiation (Andrews et al., 1993; Igarashi et al., 1994; Oyake et al., 1996; Motohashi et al., 2000; Brand et al., 2004; Tahara et al., 2004a, 2004b). In diverse types of cells, MafK-Bach1 represses expression of subset of oxidative stress-inducible genes such as heme oxygenase-1 (HO-1) and ferritins (Sun et al., 2002, 2004; Igarashi and Sun, 2006; Hintze et al., 2007), whereas heterodimer of MafK and NF-E2-related factor 2 (Nrf2) activates their expression (Itoh et al., 1997; Zhang et al., 2006). In B cells, MafK-Bach2 heterodimer represses the transcription of Blimp-1 gene, a master regulator of plasma cell differentiation (Muto et al., 1998, 2004; Ochiai et al., 2006, 2008). Small Maf heterodimers bind to their target genes by recognizing specific DNA sequences termed Maf recognition

elements (MAREs) (Kataoka et al., 1995). However, molecular mechanisms by which these heterodimers repress or activate target genes are still unclear.

We purified MafK complex from mouse plasmacytoma cell line X63/0 with an aim to understand its protein network. MATIIα was identified in the purified MafK complex by mass spectrometry analysis. We further purified MATIIα, revealing its interaction with components of Polycomb group (PcG), NuRD, Swi/Snf, and PARP complexes. We demonstrated that both MATIIα and MATIIβ were recruited to MARE of the HO-1 gene. The enzymatic activity of MATIIα, as well as its interacting proteins including MATIIβ and CHD4, was required for the HO-1 repression. Purified MATIIα associating with MATIIβ and other factors catalyzed SAM synthesis and histone methylation in vitro. Therefore, MATIIα and -β within this higher-order oligomer were named a SAM-integrating transcription regulation (SAMIT) module. We suggest that MATII serves as a transcription corepressor of MafK by providing SAM locally and interacting with chromatin-related factors.

RESULTS

Proteomic Analysis of MafK Network

To understand the protein network involving MafK, we purified MafK complexes from mouse plasmacytoma (X63/0) cells stably expressing FLAG-HA-His epitope-tagged MafK (eMafK). The expression level of eMafK in X63/0 cells was similar to that of endogenous MafK (data not shown). eMafK was purified from nuclear extracts by two-step immunoaffinity chromatography (see the Experimental Procedures; Figure 1A, lane 2). As a control, we performed a mock purification from nuclear extracts prepared from nontransduced X63/0 cells (Figure 1A, lane 1). As shown in Figure 1A, the purified eMafK fraction contained several other proteins at varying stoichiometric ratios. We employed mass spectrometry to identify these proteins. The presence of Bach1 and endogenous MafK verified the purification procedure because MafK forms a heterodimer with Bach1 or a homodimer (Table S1, Figures 1A and 1B). There were at least 11 bands that appeared specific because they were present in several independently purified samples but were absent in mock purification. A list of identified proteins is provided as Table S1, available online. MafK-interacting proteins included facilitates chromatin transcription (Supt16h/Fact140), poly(adenosine diphosphate-ribose) polymerase-1 (PARP1), Ku80, Ku70, and MATIIα. The presence of identified proteins including MATIIα in the MafK complex was confirmed by immunoblot analysis (Figure 1B). Using the Bach1 complex purified and characterized from murine erythroleukemia (MEL) cells (Dohi et al., 2008), we found that MATIIα was present in this complex by mass spectrometry and immunoblot analyses (Figure 1C and data not shown). To verify the specificity of MafK-MATIIα interaction, we carried out an immunoprecipitation analysis of endogenous proteins in mouse hepatoma (Hepa1) cells (Figure 1D) and found that MATIIα was coimmunoprecipitated with MafK (Figure 1D, middle panel). The expression of MATIIα was detected in X63/0 plasmacytoma cells, MEL, Hepa1 cells, and murine embryonic fibroblasts (MEFs), showing a wide distribution (Figure S1). These results raised the possibility that MATIIα interacted directly or indirectly with MafK and/or Bach1 in various tissues or cells.

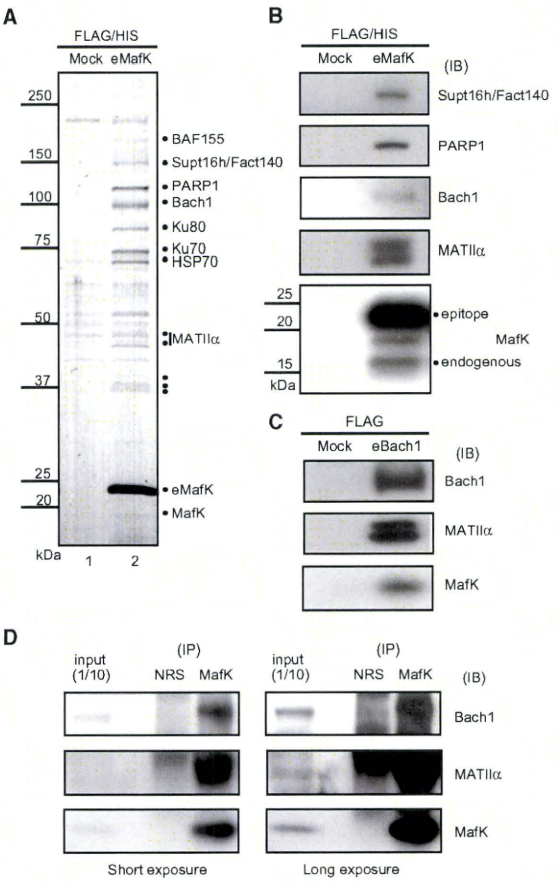

Figure 1. Purification of MafK Complex

(A) MafK complexes were affinity purified from nuclear extracts prepared from X63/0 cells expressing eMafK. Mock purification was used as a control. Specific and reproducible bands are indicated with dots.

(B) An immunoblot (IB) analysis of the affinity-purified samples (derived from A) using indicated antibodies. Epitope-tagged and endogenous MafK are shown with dots.

(C) An immunoblot (IB) analysis of the affinity-purified Bach1 complex in MEL cells using indicated antibodies.

(D) Interaction of MafK with MATIIα in Hepa1 cells. Whole-cell extracts of Hepa1 cells (left lanes as an input) were immunoprecipitated with anti-MafK antibody (right lanes) or normal rabbit serum (NRS; middle lanes). The immunoprecipitates were then immunoblotted with indicated antibodies. Short (left) or long (right) exposures are shown.

Subcellular Localization of MATIIα

To elucidate where MATIIα localizes in a cell, we carried out an immunofluorescence confocal microscopy analysis using X63/0, MEL, and simian virus 40-transformed human fibroblast (GM02063) cells. Individual cells were classified into three

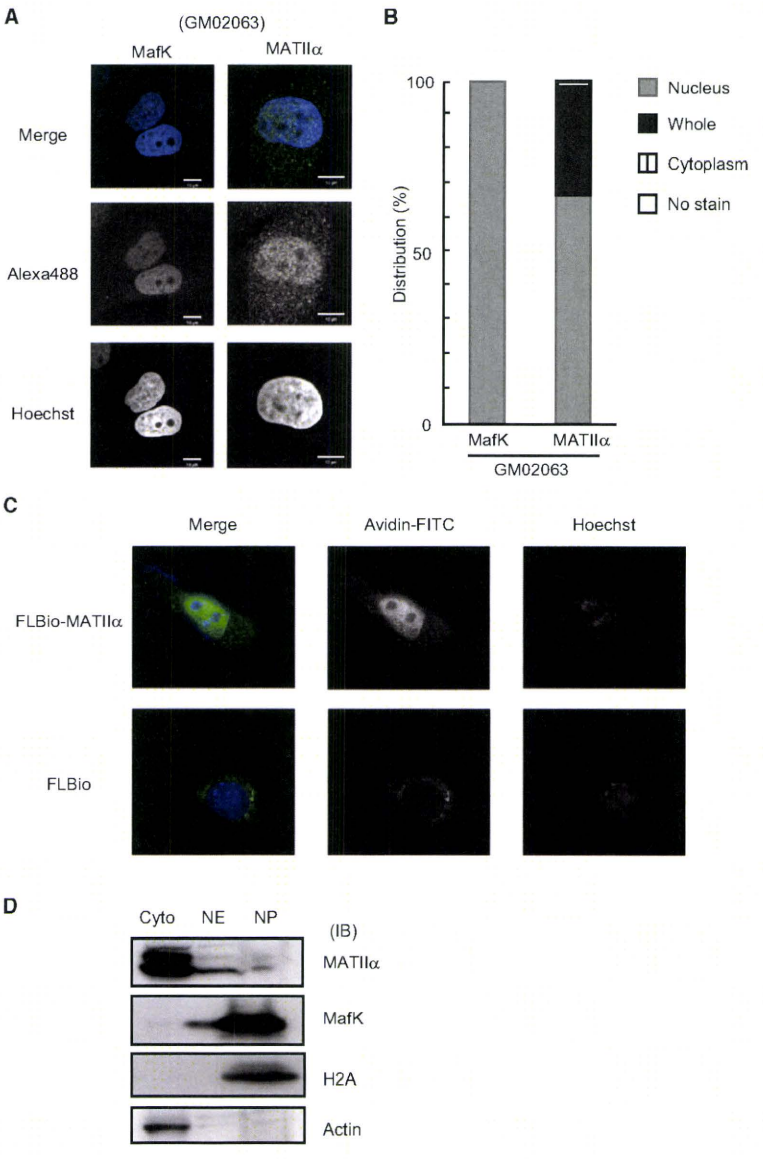

Figure 2. Subcellular Localization of MafK and MATIIα

(A) MafK (left) and MATIIα (right) in GM02063 cells were detected by the immunostaining with anti-MafK or MATIIα antibodies. DNA was stained by Hoechst. Merged images show MafK or MATIIα (green) and DNA (blue).

(B) One hundred GM02063 cells stained with anti-MATIIα antibodies were classified into four different categories: nucleus-dominant (gray box), nucleus and cytoplasm (black box), and cytoplasm-dominant (stripe box) staining of MATII.

(C) FLBio-MATIIα (upper panel) was detected with streptavidin-FITC in Hepa1 cells. DNA was stained by Hoechst. Merged images show FLBio-MATIIα (green) and DNA (blue). FLBio plasmid was used as a control (lower panel).

(D) Cytoplasmic (Cyto), nuclear extracts (NE), and nuclear pellet (NP) of MEL cells were analyzed by immunoblotting using indicated antibodies. H2A and actin served as controls for NP and Cyto, respectively.

categories depending on the localization of MATIIα signal: cytoplasmic-dominant, nuclear-dominant, or diffuse distribution. We found that endogenous MATIIα localized in not only cytoplasm but also nucleus of GM02063 (Figures 2A and 2B), X63/0 (Figures S2A and S2C), and MEL (Figures S2B and S2D). As a verification, we next used cells expressing MATIIα tagged with a biotin ligase sequence (FLBio-MATIIα). FLBio-MATIIα or parent FLBio plasmids were transfected in Hepa1 cells together with BirA (biotin-protein ligase). The subcellular localization of MATIIα was detected with streptavidin-conjugated FITC. MATIIα localized predominantly in nucleus (Figure 2C). Upon biochemical fractionation of subcellular compartments of MEL cells, endogenous MATIIα was found in not only cytoplasmic extracts but also nuclear extracts (Figure 2D). A small fraction was found in the insoluble nuclear pellets that contained chromatin including histone H2A. In contrast to the above results, however, more intense MATIIα signal was found in cytoplasmic extracts. While this may be due to leakage during the fractionation procedure, the exact reason is not clear at present. MafK was found mainly in the chromatin fraction (Figure 2D). These results indicated that a fraction of MATIIα was localized in the nuclear compartment of cells.

Proteomic Analysis of MATIIα-Interacting Proteins

To gain insight into the nuclear function of MATIIα, we purified MATIIα-interacting proteins from nuclear extracts of MEL cells stably coexpressing FLBio-MATIIα and BirA. The expression level of FLBio-MATIIα in MEL cells was similar to that of endogenous MATIIα (Figure S3A). The FLBio-MATIIα biotinylated by BirA was purified from nuclear extracts by biotin-avidin affinity chromatography (Figure 3A, lane 2). As a control, we performed a mock purification from nuclear extracts prepared from MEL cells expressing only BirA (Figure 3A, lane 1). The purified FLBio-MATIIα fraction contained many other proteins at varying stoichiometric ratios.

We employed mass spectrometry to identify the MATIIα-associating proteins. To exclude nonspecific proteins, we also carried out mass spectrometry of the mock samples in parallel.

By comparing two sets of data, there were at least 127 proteins that appeared specific because they were present in three independently purified MATIIα samples but not in three independent samples from mock purification. The complete list of identified proteins is provided as Table S2. The MATIIα-interacting proteins included many proteins with known nuclear functions (Figure 3B). Gene ontology (GO) terms such as transcriptional repression, chromatin assembly and remodeling, and DNA repair and replication were prevalent. The interaction of identified proteins with MATIIα was confirmed by immunoblot analysis (Figure 3C). Among candidate proteins examined, only one protein was not confirmed (data not shown), corroborating the specificity of mass spectrometry analysis. The presence of Bach1 and MafK verified the purification procedure (Figure 3C). The presence of MATIIβ suggested its nuclear function with MATIIα. Some of the interacting proteins belong to the PcG complex (Ring1A, Ring1B, and Yy1), NuRD complex (MTA1, CHD3, CHD4, and RbAp48), Swi/Snf complex (BAF180, BAF155, BAF57, BAF53a, and BAF47), CHRAC complex (ACF1), Sin3 complex (Sin3a), and PARP complex (Supt16/Fact140 and PARP1) (Figures 3B and 3C). To compare MATIIα-interacting proteins with those of MafK under the same condition, we purified MafK from MEL cells using the in vivo biotinylation system and found additional MafK interactors (Figure S3B). Importantly, 13% of these proteins were identified in the MATIIα-interacting proteins (Figures 1A and 3B–3D, Figure S3B, and Tables S1 and S2). These results strongly suggest that MATIIα is involved in the regulation of gene expression by interacting with transcription factors and epigenetic regulators.

Derepression of HO-1 in MATIIα Knockdown

HO-1, one of the MafK target genes, is repressed by MafK/Bach1 heterodimer that binds to MAREs within the two enhancers (E1 and E2) (Figure 4A). To explore MATIIα function in the regulation of HO-1, we carried out transient knockdown of MATIIα with small interfering RNA (siRNA 604 and 911) in mouse hepatoma (Hepa1) cells. RT-PCR and immunoblotting analyses revealed that MATIIα mRNA and protein remained low for 72 hr after introduction of siRNA (Figures S4A and S4B). Expression of MATI/III, Bach1, β-actin, and α-tubulin (Tuba 4) was not affected by the MATIIα-targeted siRNA (Figures S4A and S4B), confirming the specificity of knockdown. A 3 day (72 hr) incubation with siMATIIα resulted in significant elevation of mRNAs of HO-1 and other MafK target genes, ferritin light-chain, ferroportin, glutathione S-transferase μ1 (GSTμ1), and GSTμ3 (Figure 4B, Figures S4C and S4D). In contrast, ferritin heavy-chain (FTH), NAD(P)H quinone oxidoreductase 1 (NQO1), GSTα4, glutamate-cysteine ligase modifier subunit (GCLM), and glutamate-cysteine ligase catalytic subunit (GCLC) were not affected significantly (Figures S4C and S4D).

The expression of HO-1 was also elevated by treating cells with Bach1 siRNA (siBach1) (Figure S4E), suggesting that MATIIα functioned with MafK-Bach1 heterodimer. Transcription of HO-1 and other MafK target genes is induced in response to diverse stresses including oxidative stress (Keyse and Tyrrell, 1989; Ishii et al., 2000). To determine whether MATIIα was involved in the tuning of inducible expression, we treated Hepa1 cells by adding diethyl maleate (DEM), an oxidative stress inducer, to the culture medium (Figure 4B). Induction of HO-1 was evident in control cells within 4 hr after 100 μM DEM treatment and reached a maximum level by 8 hr (Figure S4F). Upon MATIIα knockdown, HO-1 induction became exaggerated as compared with the control cells (Figure 4B and Figure S4F). It was enhanced upon Bach1 knockdown as well (Figure S4E). Induction of FTL by DEM was also enhanced upon MATIIα knockdown (Figure S4C).

We examined an effect of MATI/III siRNA (siMATI/III) upon expression of MafK target genes and found that expression of HO-1, FTH, FTL, and GSTμ3 was not affected under normal or oxidative conditions (Figures S4G and S4H). Thus, we concluded that the MafK-related function was specific to MATIIα among the isozymes.

MATIIα Recruitment to the Maf Recognition Element of HO-1 Gene

To further elucidate the nuclear function of MATIIα in terms of MafK complex, we asked whether MATIIα was recruited to the target genes of MafK. We performed chromatin immunoprecipitation (ChIP) assays in X63/0 cells using anti-MAT antibody which recognizes MATIIα and MATI/III, because there is no MATIIα-specific antibody that can be used in a ChIP assay as far as we could determine. Crosslinked chromatin fragments of X63/0 cells were immunoprecipitated using anti-MafK or MAT antibodies, and the two enhancers (E1 and E2) and promoter of HO-1, and the promoter of a neighboring gene Mcm5 were examined and quantified by PCR for relative enrichment (Figures 4C and 4D). MATIIα bound to the E1 enhancer, whereas MafK bound to the three regulatory regions of HO-1.

To further investigate MATIIα binding to HO-1 gene, we utilized FLBio-MATIIα. FLBio-MafK was used as a positive control. Crosslinked chromatin fragments of Hepa1 cells were incubated and pulled down with streptavidin beads (ChPD) (Figures 4E–4I). Among the regions examined, E1 and E2 enhancers of HO-1 were specifically enriched by streptavidin beads from the chromatin of cells expressing biotinylated MATIIα, but not from those expressing BirA alone (Figures 4F–4I, each minus [–] columns). Binding of biotinylated MATIIα, but not of endogenous MATIIα to the HO-1 E2, may reflect differences in the sensitivities of the assays, including epitope accessibilities. Interestingly, the recruitment of biotinylated MATIIα to these enhancers decreased in response to DEM treatment (Figure 4E, right, and Figures 4F–4I, each plus [+] columns), consistent with the repressive function of MATIIα. While we found that biotinylated MafK bound to E1, E2, and promoter of HO-1, binding to the enhancers was higher than the promoter (Figures 4F–4H). This may suggest that the specific recruitment of biotinylated MATIIα to E1 and E2 was mediated by MafK. These results indicate that not only MafK but also MATIIα bound specifically to the HO-1 gene and suggest a specific role for MATIIα in transcription regulation. In addition, departure of MATIIα upon oxidative stress may be a critical step for the HO-1 induction.

Modification of Histone H3 at the HO-1 Locus

Considering the fact that MATIIα synthesizes SAM required for histone and DNA methylation, we hypothesized that knockdown of MATIIα affected repressive methylation at the HO-1 chromatin

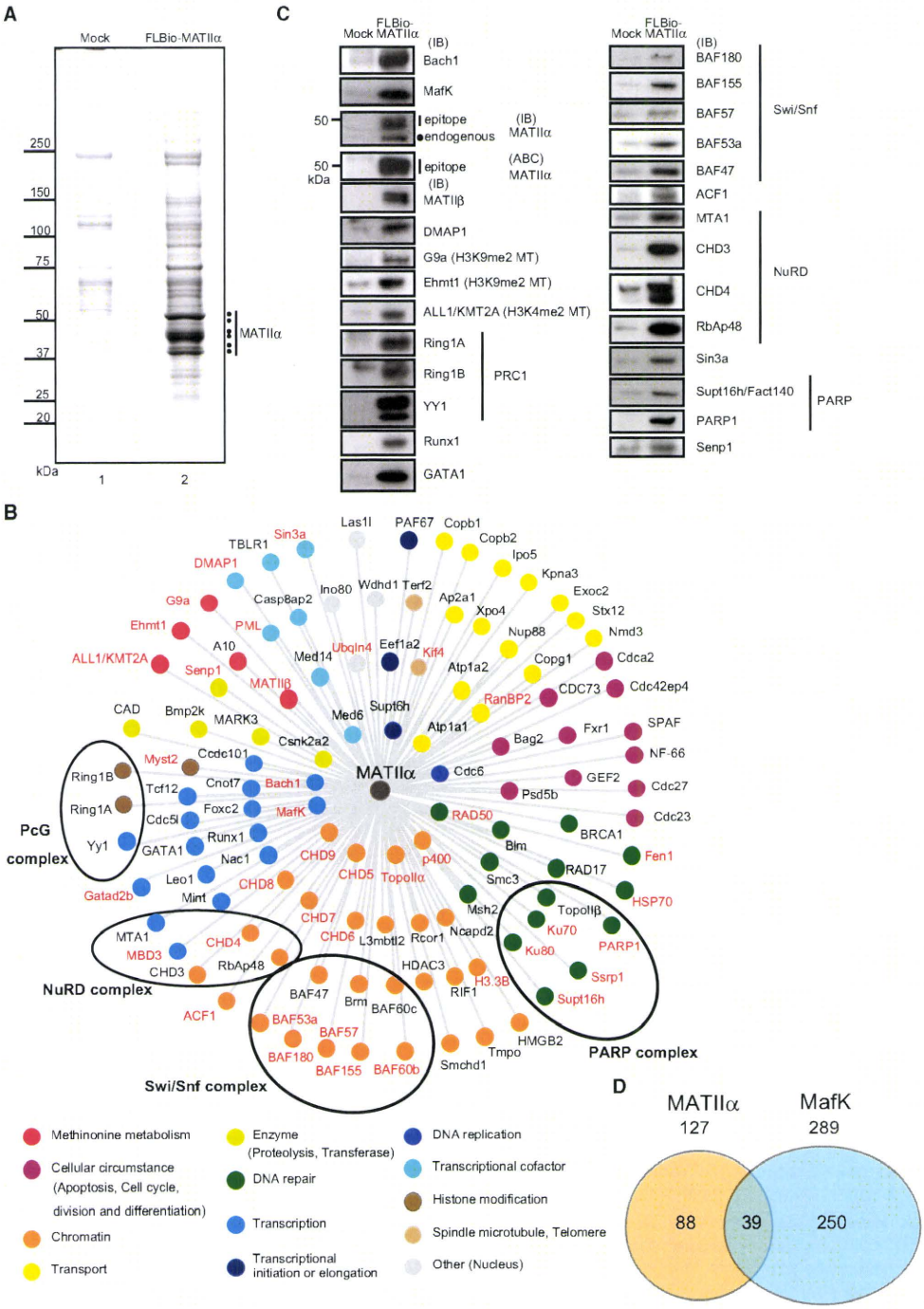

Figure 3. Purification of MATIIα-Associating Proteins

(A) MATIIα was affinity purified from MEL cells stably coexpressing FLBio-MATIIα and BirA. Purification from cells expressing only BirA (mock) was used as a control. MATIIα bands are indicated with dots.

domain. To investigate this possibility, we examined the degree of repressive modification (i.e., trimethyl and dimethyl K9 [H3K9 me3 and me2] and trimethyl K27 [H3K27 me3]) and activating modifications (i.e., dimethyl K4 [H3K4 me2], acetyl K9 [H3K9 Ac], acetyl K27 [H3K27 Ac], and trimethyl K36 [H3K36 me3]) of histone H3 at HO-1 locus using ChIP (Figures 5A–5C). There was no detectable level of H3 K9 and K27 me3 at the HO-1 locus (Figure 5A). In contrast, H3K9 me2 was clearly observed at the E1 region (Figure 5C). As previously reported for NIH 3T3 cells (Sun et al., 2004), histone H3K4 at the enhancers (E1 and E2) and promoter of HO-1 was hypermethylated under normal culture condition (Figure 5A). Upon MATIIα knockdown, H3K4 me2 and H3K9 me2 decreased (Figures 5A–5C). H3K36 me3, linked to transcriptional elongation, was detected at the exon 3 region of HO-1 in both control and MATIIα knockdown cells (Figure 5A). There are CpG islands in the E2 and promoter regions of HO-1 (data not shown). We examined CpG methylation in these regions by bisulphite genomic sequencing. The E2 and promoter regions of HO-1 were found devoid of CpG methylation under normal conditions (Figure S5A). Taken together with a recent report that H3K4 me2 recruits the Set3 histone deacetylase complex to suppress nucleosome acetylation and remodeling (Kim and Buratowski, 2009), these observations suggest that the repression of HO-1 by MATIIα may involve the H3K4 me2 and H3K9 me2 marks.

Catalytic Activity of MATIIα Involved in the Repression of HO-1

To investigate whether the catalytic activity of MATIIα is required to repress HO-1, we constructed a mutated MATIIα (MATIIα D134A) converting aspartic acid of amino acid 134 to alanine. MAT enzymes possess an evolutionary conserved common ATP binding motif (GXGDXG) (Figure S5B). A mutation of the aspartic acid within this motif of human MATI/III almost completely abolishes the catalytic activity (Chamberlin et al., 2000, and Figure S5B). We treated Hepa1 cells expressing wild-type MATIIα or MATIIα D134A by adding DEM and compared the relative expression of HO-1 with control cells (Figure 5D). Upon overexpression of MATIIα D134A, induction of HO-1 mRNA became exaggerated as compared with the control cells (Figure 5D). Overexpression of wild-type MATIIα did not show such a stimulatory effect (Figure 5D). These data indicated that the enzymatic activity of MATIIα was required for the repression of HO-1 by MafK and Bach1.

The dominant-negative effect of MATIIα D134A upon HO-1 regulation suggested that a simple lack of SAM was not the cause of HO-1 derepression upon MATIIα knockdown. To test this idea, we treated cells with both siMATIIα and ectopic SAM. The derepression of HO-1 with siMATIIα was not reversed by adding SAM (Figure 5E). Together with the results that MATIIα D134A showed a dominant-negative effect, the repression of HO-1 may require a local supply of SAM by MATIIα.

MATIIα-Associating Factors Involved in the Repression of HO-1

Among the MATIIα-associating proteins (Figure 3), we chose several proteins that were known to play roles in gene repression and MATIIβ to investigate their involvement in HO-1 repression. BAF53a, CHD4, or MATIIβ knockdown (siBAF53a, siCHD4, or siMATIIβ) resulted in derepression of HO-1 under normal conditions (Figure 6A and Figures S6A and S6B). E1 and E2 enhancers and promoter of HO-1 were specifically enriched by anti-BAF53a, anti-CHD4, or anti-MATIIβ antibodies (Figure 6B), showing their binding to the HO-1 regulatory regions. Recruitment of BAF53a and CHD4 to the HO-1 locus was not abolished upon MATIIα knockdown (Figure S6C), indicating that MATIIα was not required for their recruitment. PARP1 knockdown also resulted in HO-1 derepression under the presence of oxidative stress (Figure 6C and Figures S6A and S6B).

Association of Methyltransferase Activity with MATIIα

The involvement of both the catalytic activity of MATIIα and its interacting factors in the HO-1 repression suggested that these factors might further interact with methyltransferases. To investigate this possibility, methyltransferase activity associated with MATIIα was determined by a conventional histone methyltransferase (HMT) assay. Recombinant G9a and FLBio-MATIIα fraction affinity purified from MEL cells using avidin beads showed methylation activities toward histone H1 and H3, whereas the corresponding fraction purified from control cell (mock) contained significantly less activity (Figures 7A–7C).

The copurification of MATIIα and HMT activities suggested that SAM synthesis and methylation might be coupled by their physical interaction. To investigate this possibility, we developed a new HMT assay involving synthesis of SAM from methionine and ATP (MAT-HMT assay). The affinity-purified FLBio-MATIIα fraction, without any extraneous methyltransferase added, showed methylation activity toward histone H1 and H3, and this activity was dependent on ATP (Figures 7D–7F). In contrast, recombinant G9a and mock fraction did not modify histones (Figure 7D). These results strongly suggested that MATIIα associated with histone H1 and H3 methyltransferases in the nuclei.

To characterize the relationship among MATIIα, MATIIβ, BAF53a, CHD4, PARP1, and HMT activities, we obtained MATIIα-enriched materials by single anti-FLAG affinity purification of biotinylated FLBio-MATIIα from MEL cells, and fractionated them using 10%–35% (v/v) glycerol gradient sedimentation. Whereas MATIIα and β subunits formed peaks corresponding to around 158 kDa, substantial portions of them sedimented much faster, indicating the presence of a high-molecular-mass form of roughly 640 kDa (Figure 7G). MATIIα may form several different complexes, or associations of the complex components may be fragile. BAF53a, CHD4, Bach1, and MafK were found in the relatively faster-sedimenting fractions (Figure 7G). PARP1 presumably modified by poly-ADP-ribosylation was also present

(B) MATIIα-associated proteins were categorized by gene ontology (GO) annotations as listed in the *Mus musculus* Genome Database. Known protein complexes are denoted by black circles. Proteins found in the MafK complex (Figure S4) are shown in red. Those found in the MafK complex in Figure 1 are shown in bold.
(C) Immunoblot (IB) analysis of the affinity-purified samples (derived from A) using indicated antibodies or by a biotin-avidin complex (ABC) analysis (FLBio-MATIIα).
(D) Venn diagram of proteins associated with FLBio-MATIIα or FLBio-MafK in MEL cells.

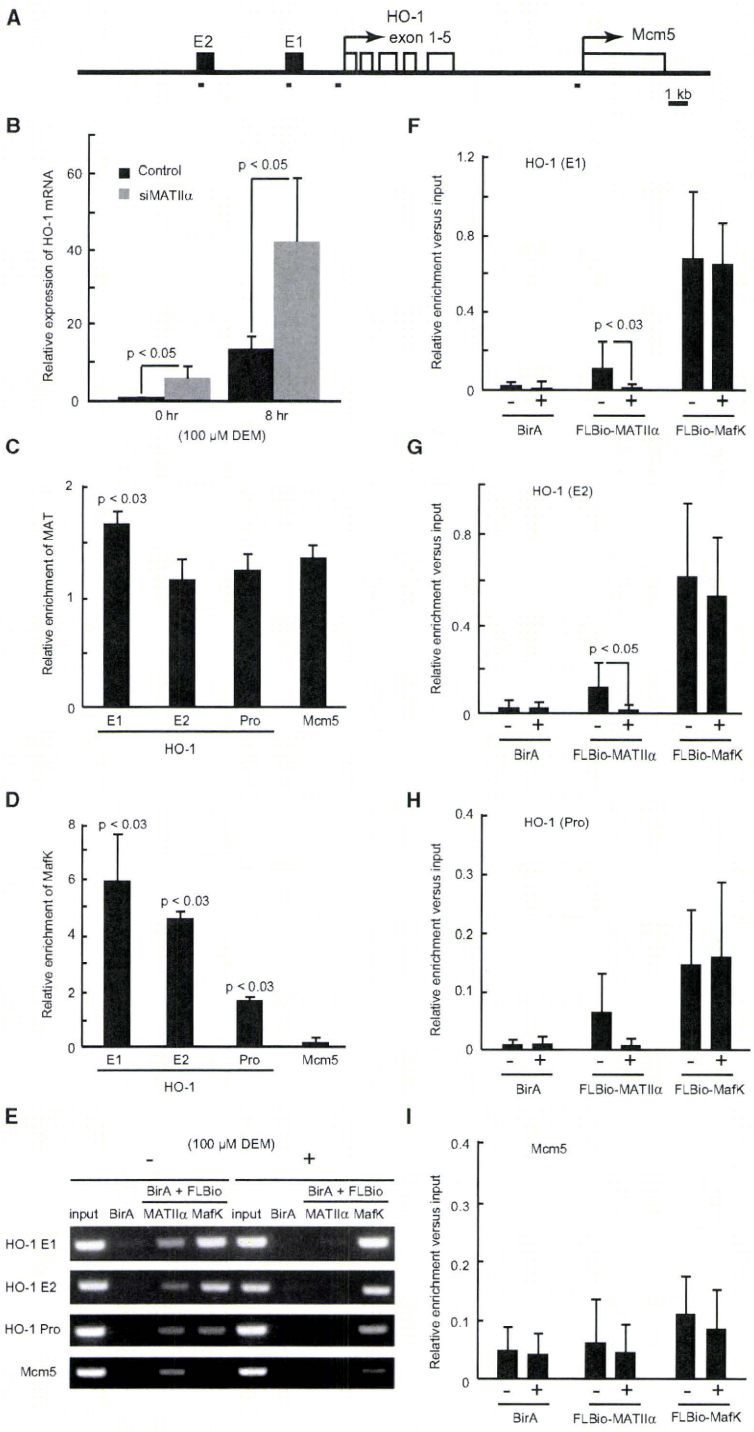

Figure 4. MATIIα Recruitment to HO-1 Locus

(A) Schematic representation of mouse HO-1 and Mcm5 loci. Lines below indicate PCR primer pairs for ChIP and ChPD analyses.

(B) Quantitative RT-PCR (qRT-PCR) analysis of HO-1 mRNA in Hepa1 cells with control (black) and MATIIα siRNA (gray). Cells were treated with or without 100 μM DEM for 8 hr. The expression level of HO-1 gene in control under normal condition was arbitrarily set at 1. β-actin mRNA measurement was used to normalize the results. The averages of three independent experiments with standard deviation are shown. P values (Student's t test) for differences between control and MATIIα siRNA are indicated.

(C and D) ChIP assays were performed by using antibodies to MAT (C) or MafK (D) with X63/0 cells. Relative levels of enrichment of each genomic DNA region compared to control IgG are shown. These results represent three independent experiments with standard deviation. P values (Student's t test) for differences between MAT (C) or MafK (D) and control rabbit IgG signals are indicated.

(E) ChPD assays were performed with Hepa1 cells coexpressing FLBio-MATIIα or FLBio-MafK and BirA. Cells expressing only BirA were examined as a control. Cells were treated with or without 100 μM DEM for 8 hr. Gel images of PCR products of indicated regions are shown.

(F–I) ChPD assays were performed as above and quantified. Relative levels of enrichment of the indicated genomic regions are shown. These results represent three independent experiments with standard deviation. P values (Mann-Whitney U test) for differences between cells treated with or without DEM are indicated.

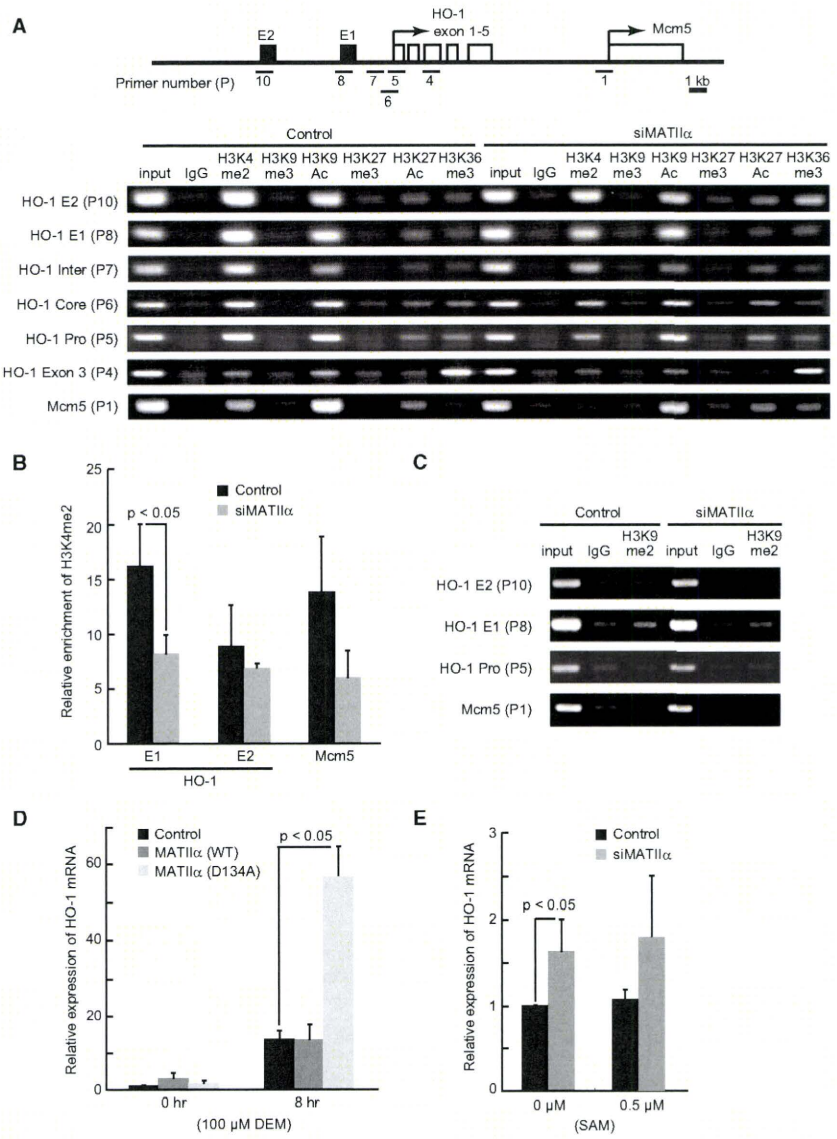

Figure 5. Enzymatic Activity of MATIIα and Repression of HO-1

(A) Schematic representation of mouse HO-1 and Mcm5 loci (upper). Primers used to amplify various genomic regions are also shown. Cells were treated with control or MATIIα siRNA, and ChIP assays were performed using indicated antibodies (lower).

(B) Relative levels of dimethylated histone H3 (K4 me2) at indicated genomic regions in Hepa1 cells treated with control (black) or MATIIα siRNA (gray). The averages of three independent experiments with standard deviation are shown. P value (Student's t test) for differences is indicated.

(C) Dimethylated H3K9 at HO-1 locus. ChIP assays were performed as in (A) using dimethylated histone H3 (K9 me2) antibody.

(D) qRT-PCR analysis of HO-1 mRNA in control cells (black) or those overexpressing wild-type MATIIα (gray) or MATIIα D134A (light gray). These cells were treated with DEM for 8 hr. The averages of three independent experiments with standard deviation are shown. The expression level of HO-1 gene in control under normal condition was arbitrarily set at 1. β-actin mRNA measurement was used to normalize the results.

(E) qRT-PCR analysis of HO-1 mRNA in cells treated with control (black) or MATIIα siRNA (gray). Cells were treated with or without 0.5 μM SAM for 12 hr.

in these fractions. We pooled respective fractions to compare the smaller and larger MATIIα fractions in detail (S1 and S2 in Figure 7G) and carried out further purification using biotin-avidin affinity chromatography (Figure 7H). Whereas BAF53a, Bach1, and MafK interacted with MATIIα in both fractions, interaction of CHD4 was found mainly in the larger fractions (Figure 7H).

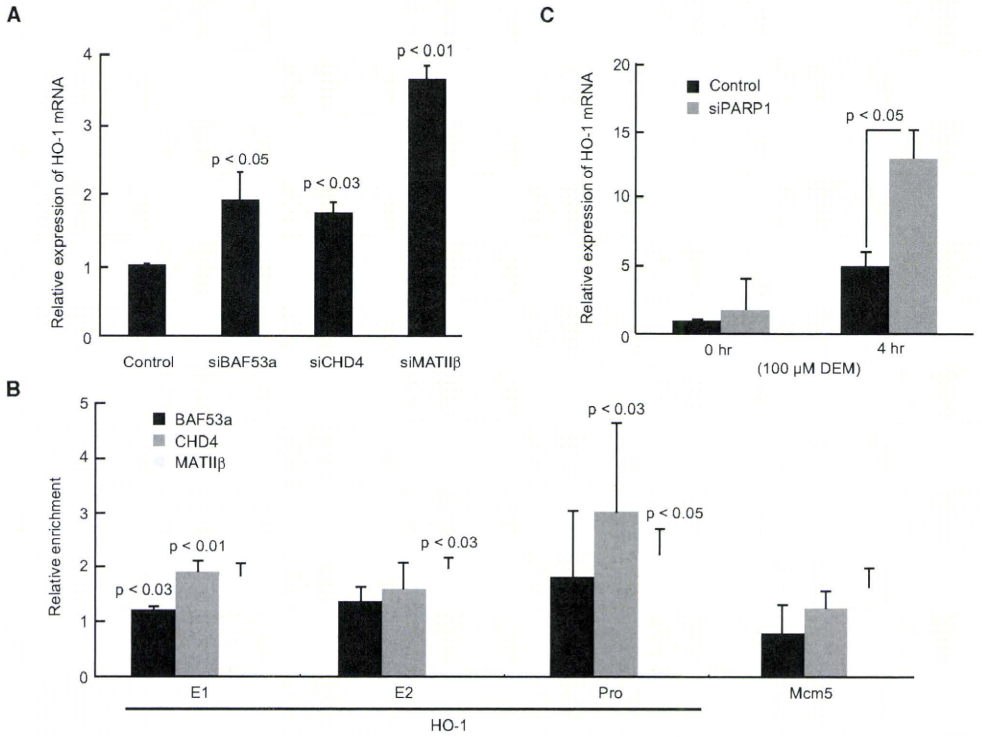

Figure 6. MATII-Associating Factors Repress HO-1 Expression

(A) qRT-PCR analysis of HO-1 mRNA in Hepa1 cells treated with control, siBAF53a, siCHD4, or siMATIIβ. Error bars represent standard deviation.

(B) BAF53a, CHD4, and MATIIβ were recruited to HO-1 locus. ChIP assays were performed using indicated antibodies. Relative levels of enrichment of indicated genomic DNA regions are shown with standard deviation. P values (Student's t test) for differences between specific antibodies and control rabbit IgG signals are indicated.

(C) qRT-PCR analysis of HO-1 in cells treated with control (black) or PARP1 siRNA (gray). Cells were treated with or without 100 μM DEM for 4 hr.

Interaction of PARP1 was hardly detected in either fraction (data not shown), suggesting that its interaction with MATIIα was labile and lost. The two forms of MATIIα were examined for SAM synthesis and histone methylation in MAT-HMT assay (Figure 7I). We found that only the high-molecular-mass form of MATIIα and its interacting proteins purified from the larger fractions showed SAM synthesis-dependent methylation activity toward histone H1 and H3 (Figure 7I). These results suggest that biosynthesis of SAM is physically coupled with histone methylation on chromatin (Figure 7J).

DISCUSSION

While SAM is essential for histone and DNA methylation, little is known about the function of MATIIα in the context of gene and chromatin regulation. A previous report identified MATIIα as a modifier mutation of chromatin architecture (Larsson et al., 1996). In *Drosophila melanogaster*, modifier mutations of position-effect variegation and PcG genes have been useful tools to investigate genes involved in chromatin architecture. Suppressor of zeste 5 (Su[z]5) encodes MATIIα and acts as enhancers of Polycomb (i.e., reduced activity of both MATIIα and Polycomb resulting in chromatin derepression), suggesting that MATIIα is involved in the process of gene silencing in fly (Larsson et al., 1996). However, this historical study has not been followed up as far as we know, and mechanistic defects in the Su(z)5 mutant are not known. We have extended this study and revealed the molecular function of MATIIα by proteomics analyses of MafK, Bach1, and MATIIα (Figures 1 and 3).

We showed that a fraction of MATIIα was localized in the nuclear compartment of various cells (Figure 2). We also found that MATIIα was recruited to MARE of enhancers at HO-1 locus in X63/0 and Hepa1 cells (Figures 4C and 4E–4I). Upon MATIIα knockdown, mRNA and protein levels of HO-1 were elevated and further induced strongly upon DEM treatment (Figure 4B and data not shown). MATIIα knockdown showed similar effects upon some other MafK target genes (Figures S4C and S4D). These observations suggest collectively that MATIIα functions as a corepressor of MafK and Bach1.

The purification of MATIIα from MEL cells provided strong evidences for its functions around chromatin. MATIIα was